

NOV 23 1946

ACR No. L5F27

NATIONAL ADVISORY COMMITTEE FOR AERONAUTICS

WARTIME REPORT

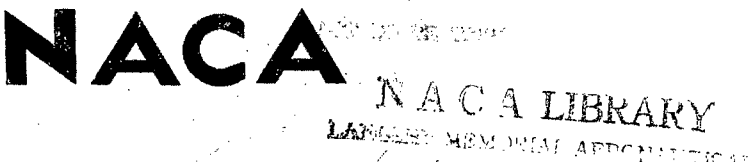
ORIGINALLY ISSUED

December 1945 as
Advance Confidential Report L5F27

TWO-DIMENSIONAL WIND-TUNNEL INVESTIGATION OF
0.20-AIRFOIL-CHORD PLAIN AILERONS OF DIFFERENT
CONTOUR ON AN NACA 65₁-210 AIRFOIL SECTION

By William J. Underwood, Albert L. Braslow,
and Jones F. Cahill

Langley Memorial Aeronautical Laboratory
Langley Field, Va.



WASHINGTON

NACA WARTIME REPORTS are reprints of papers originally issued to provide rapid distribution of advance research results to an authorized group requiring them for the war effort. They were previously held under a security status but are now unclassified. Some of these reports were not technically edited. All have been reproduced without change in order to expedite general distribution.

NACA ACR No. L5F27

NATIONAL ADVISORY COMMITTEE FOR AERONAUTICS

ADVANCE CONFIDENTIAL REPORT

TWO-DIMENSIONAL WIND-TUNNEL INVESTIGATION OF
0.20-AIRFOIL-CHORD PLAIN AILERONS OF DIFFERENT
CONTOUR ON AN NACA 65₁-210 AIRFOIL SECTION

By William J. Underwood, Albert L. Braslow
and Jones F. Calkill

SUMMARY

An investigation was made of three interchangeable sealed-gap 0.20-airfoil-chord plain ailerons of different contour on the NACA 65₁-210 airfoil section. The three aileron contours tested were the true airfoil contour, straight sides, and a beveled trailing edge. The effects of aileron contour on the section aerodynamic characteristics of the airfoil and aileron are presented herein.

The results of the tests indicated that thickening or beveling the aileron trailing edge by the amount investigated would decrease the aileron effectiveness, the rate of change of section lift coefficient with section angle of attack, and the maximum section lift coefficient; would increase positively the rate of change of section hinge-moment coefficient with both section angle of attack and aileron deflection; would shift the aerodynamic center forward; and would cause no significant change in the section profile-drag coefficient with aileron neutral or in the increment of section pitching-moment coefficient induced by aileron deflection at constant lift. The balancing action of the aileron and the loss in aileron effectiveness caused by beveling the trailing edge were accentuated by the application of standard leading-edge roughness to the airfoil. The computed characteristics of the three sealed internally balanced ailerons, based on the data for the hinge-moment and seal-pressure-difference coefficients of plain ailerons, showed an appreciable effect of aileron contour on the hinge moments at the larger aileron deflections even though all three ailerons were computed to have the same hinge-moment slope at small aileron deflections.

INTRODUCTION

The use of thin airfoil sections to delay the effects of compressibility on the wings of modern high-performance airplanes has emphasized the need for data on the aerodynamic characteristics of ailerons on thin airfoils. The effects of aileron contour on the aerodynamic characteristics of ailerons have been shown previously by investigations of a limited number of airfoils equipped with control surfaces. Since very little section aerodynamic data are available for ailerons on thin NACA 6-series airfoils, tests were made of an NACA 65₁-210 airfoil equipped with three interchangeable sealed-gap 0.20-airfoil-chord plain ailerons of different contour.

The investigation was made in the Langley two-dimensional low-turbulence pressure tunnel. The three ailerons tested differ only in contour and are designated herein as true-contour, straight-sided, and beveled ailerons. The hinge moments and effectiveness of the aileron and the pitching-moment and profile-drag characteristics of the airfoil were determined. Tests were made with the airfoil surface aerodynamically smooth and with standard roughness applied to the leading edge of the airfoil. The differential pressures across the aileron seal were obtained for use in calculating the hinge-moment characteristics of ailerons having any amount of sealed internal balance.

COEFFICIENTS AND SYMBOLS

The coefficients and symbols used herein are as follows:

c_l airfoil section lift coefficient $\left(\frac{l}{q_0 c} \right)$

c_{d_0} airfoil section profile-drag coefficient $\left(\frac{d_2}{q_0 c} \right)$

$c_m c/4$ airfoil section pitching-moment coefficient about quarter-chord point $\left(\frac{m}{q_0 c^2} \right)$

$\Delta p/q_0$ seal-pressure-difference coefficient; positive when pressure below seal is greater than pressure above seal

c_h aileron section hinge-moment coefficient based on aileron chord $\left(\frac{h}{q_0 c_a^2} \right)$

c_H aileron section hinge-moment coefficient based on airfoil chord $\left(\frac{h}{q_0 c^2} \right)$

where

l airfoil lift per unit span

d_0 airfoil profile drag per unit span

m airfoil pitching moment per unit span

h aileron hinge moment per unit span; positive when aileron tends to deflect downward

c chord of airfoil with aileron neutral

c_a chord of aileron behind hinge axis

q_0 free-stream dynamic pressure $\left(\frac{1}{2} \rho_0 v_0^2 \right)$

v_0 free-stream velocity

ρ_0 free-stream density

and

α_0 airfoil section angle of attack, degrees

δ_a aileron deflection with respect to airfoil, degrees; positive when trailing edge is deflected downward

R Reynolds number

$$c_{la} = \left(\frac{\partial c_l}{\partial \alpha_0} \right)_{\delta_a}$$

$$c_{l\delta} = \left(\frac{\partial c_l}{\partial \delta_a} \right)_{\alpha_0}$$

$$c_{m_a} = \left(\frac{\partial c_m}{\partial \alpha_0} \right)_{\delta_a}$$

$$c_{m\delta} = \left(\frac{\partial c_m}{\partial \delta_a} \right)_{\alpha_0}$$

$$c_{h_a} = \left(\frac{\partial c_h}{\partial \alpha_0} \right)_{\delta_a}$$

$$c_{h\delta} = \left(\frac{\partial c_h}{\partial \delta_a} \right)_{\alpha_0}$$

$$p_\alpha = \left(\frac{\partial \Delta p}{\partial \alpha_0} \right)_{\delta_a}$$

$$p_\delta = \left(\frac{\partial \Delta p}{\partial \delta_a} \right)_{\alpha_0}$$

$$\alpha_\delta = \left(\frac{\partial \alpha_0}{\partial \delta_a} \right)_{c_l} \quad \text{aileron section effectiveness parameter}$$

$\Delta \alpha_0$ increment in airfoil section angle of attack

$\Delta \delta_a$ increment in aileron deflection

$$\left(\frac{\Delta \alpha_0}{\Delta \delta_a} \right)_{\delta_a = \pm 20^\circ} \quad \begin{array}{l} \text{aileron section effectiveness parameter} \\ (\text{ratio of increment of airfoil section} \\ \text{angle of attack to increment of aileron} \\ \text{deflection required to maintain constant lift coefficient}) \end{array}$$

$c_{h\delta_T}$ total $\frac{dc_h}{d\delta_a}$ in steady roll

n response parameter (reference 1)

$(\Delta c_h)_\delta$ increment in aileron section hinge-moment coefficient due to aileron deflection at a constant section angle of attack

$(\Delta c_h)_a$ increment of aileron section hinge-moment coefficient due to change in section angle of attack at constant aileron deflection

Δc_{H_T} increment of total aileron section hinge-moment coefficient in steady roll

$\frac{\Delta c_{H_T}}{\Delta \alpha_0 / \Delta \delta_a}$ aileron section hinge-moment parameter

The subscripts to partial derivatives denote the variables held constant when the partial derivatives were taken. The derivatives were measured at zero angle of attack and zero aileron deflection.

MODEL

The model had a 24-inch chord and a 35.5-inch span and was constructed of laminated mahogany with the exception of the interchangeable ailerons, which were constructed of solid dural (fig. 1). Ordinates of the NACA 65₁-210 airfoil section are given in table I.

The three aileron shapes tested are shown in figure 2 and consist of the true airfoil contour, straight sides, and a beveled trailing edge. The ordinates of the true-contour aileron were the same as the ordinates given in table I for the trailing-edge part of the NACA 65₁-210 airfoil section. The contours of the straight-sided and beveled ailerons were formed by straight lines as shown in figure 2. A rubber seal was used at the gap at the nose of the aileron.

For the tests of the smooth airfoil, the model was finished with No. 400 carborundum paper to produce aerodynamically smooth surfaces. For the tests of the airfoil with standard leading-edge roughness, the model

$c_{h\delta_T}$ total $\frac{dc_h}{d\delta_a}$ in steady roll

n response parameter (reference 1)

$(\Delta c_h)_\delta$ increment in aileron section hinge-moment coefficient due to aileron deflection at a constant section angle of attack

$(\Delta c_h)_a$ increment of aileron section hinge-moment coefficient due to change in section angle of attack at constant aileron deflection

Δc_{H_T} increment of total aileron section hinge-moment coefficient in steady roll

$\frac{\Delta c_{H_T}}{\Delta \alpha_0 / \Delta \delta_a}$ aileron section hinge-moment parameter

The subscripts to partial derivatives denote the variables held constant when the partial derivatives were taken. The derivatives were measured at zero angle of attack and zero aileron deflection.

MODEL

The model had a 24-inch chord and a 35.5-inch span and was constructed of laminated mahogany with the exception of the interchangeable ailerons, which were constructed of solid dural (fig. 1). Ordinates of the NACA 65₁-210 airfoil section are given in table I.

The three aileron shapes tested are shown in figure 2 and consist of the true airfoil contour, straight sides, and a beveled trailing edge. The ordinates of the true-contour aileron were the same as the ordinates given in table I for the trailing-edge part of the NACA 65₁-210 airfoil section. The contours of the straight-sided and beveled ailerons were formed by straight lines as shown in figure 2. A rubber seal was used at the gap at the nose of the aileron.

For the tests of the smooth airfoil, the model was finished with No. 400 carborundum paper to produce aerodynamically smooth surfaces. For the tests of the airfoil with standard leading-edge roughness, the model

surfaces were the same as those of the smooth airfoil except that 0.011-inch carborundum grains were applied to both surfaces at the leading edge over a surface length of $0.08c$ measured from the leading edge. This roughness is defined in reference 2 as the standard roughness for a 24-inch-chord model.

APPARATUS AND TESTS

The lift, drag, and pitching moment of the model were measured by the methods described in reference 2. The aileron hinge-moment measurements were made with electrical-resistance strain gages mounted on the beams that supported the aileron. This method of mounting eliminated the possibility of friction due to the use of bearings at the aileron hinge axis. The pressure difference across the aileron seal was measured with surface static-pressure orifices located inside the gap above and below the flexible rubber seal.

Tests of the model with each of the three ailerons were made in the Langley two-dimensional low-turbulence pressure tunnel at Reynolds numbers of 1×10^6 and 9×10^5 and at Mach numbers of 0.07 and 0.17, respectively. The tests included measurements of lift, aileron hinge moment, aileron balance pressure, and airfoil pitching moment for each aileron deflected in increments of 5° between -20° and 20° . Drag measurements were made at both Reynolds numbers through the complete range of aileron deflection for the model with the true-contour aileron and, for the models with the straight-sided and beveled ailerons, at a Reynolds number of 9×10^5 and $\delta_a = 0^\circ$ only. In addition, the model with each of the three ailerons was tested at a Reynolds number of 9×10^5 with standard roughness applied to the leading edge of the airfoil. For the airfoil with leading-edge roughness, only lift, aileron hinge moment, and aileron balance pressure were measured through the range of aileron deflections.

The following factors were applied to correct the tunnel data to free-air conditions:

$$c_l = 0.977 c_{l'}$$

$$c_{d_0} = 0.994 c_{d_0'}$$

$$q_0 = 1.006 q_0'$$

$$a_0 = 1.015 a_0'$$

where the primed quantities represent the values measured in the tunnel (reference 2).

PRESENTATION OF DATA

For use in aileron design, basic section data are presented for a range of aileron deflection in figures 3 to 9 for the true-contour aileron, in figures 10 to 15 for the straight-sided aileron, and in figures 16 to 21 for the beveled aileron. These figures include data for the airfoil with aerodynamically smooth surfaces and with standard roughness applied to the leading edge.

These basic section data may be used to predict the section hinge-moment characteristics of ailerons of similar contour and chord with any amount of sealed internal balance by the following equations:

$$\Delta c_{h_a} = \frac{\Delta p}{2q_0} \left[\left(\frac{c_b}{c_a} \right)^2 - \left(\frac{t/2}{c_a} \right)^2 \right] \quad (1)$$

$$c_{h_a \text{ balanced aileron}} = c_{h_a \text{ plain aileron}} + \Delta c_{h_a} \quad (2)$$

where

Δc_{h_a} increment in aileron section hinge-moment coefficient produced by an internal-balance arrangement

c_b chord of overhang from aileron hinge axis to middle of sealed gap

c_a chord of aileron behind hinge axis

t twice nose radius of plain aileron

Equation (1), in which the overhang is assumed to extend to the middle of the gap, can be used for determining the overhang moments of sealed internally balanced ailerons of normal configuration, that is, ailerons for which the overhang extends straight forward into the balance chamber and the sealed gap width is small.

The data obtained at a Reynolds number of 1×10^6 are not so accurate as those obtained at a Reynolds number of 9×10^6 because of the small dynamic pressure. The results for the lower Reynolds number, however, are believed to be useful for indicating qualitative effects of Reynolds number on the aileron characteristics in the range of Reynolds number from 1×10^6 to 9×10^6 .

The effects of aileron contour on section characteristics are compared by means of section parameters. Variations of these parameters and coefficients with other independent variables are presented in graphical and tabular form.

The following discussion refers to the data obtained at a Reynolds number of 9×10^6 with the airfoil surfaces aerodynamically smooth unless otherwise stated.

DISCUSSION

Aileron Effectiveness

The effects of aileron contour are shown in table II for the aileron section effectiveness parameter a_3 and for $c_{l\delta}$ and in figure 22 in which a_3 is plotted against δ_a at a constant c_l . Thickening or beveling the trailing edge of the aileron resulted in a decrease in both a_3 and $c_{l\delta}$. The value of the effectiveness parameter a_3 of each of the three ailerons tested was slightly greater than the value (-0.450) obtained for a 0.20c plain aileron of true airfoil contour on an NACA 0009 airfoil section (reference 3). The percent loss in a_3 due to trailing-edge modifications to the true-contour aileron is given in the following table:

Aileron	Airfoil	
	Smooth	Rough
True-contour	0	4.7
Straight-sided	1.5	4.7
Beveled	2.5	12.1

The value of the effectiveness parameter $\left(\frac{\Delta a_0}{\Delta \delta_a} \right)_{\delta_a = \pm 20^\circ}$

when measured over a range of aileron deflection of $\pm 20^\circ$ at a constant section lift coefficient of 0.20 was greater for the straight-sided aileron on the airfoil with a smooth surface or with leading-edge roughness than for the other two ailerons. The value of this parameter for the beveled aileron was also greater than for the true-contour aileron with the airfoil smooth but was lower with standard leading-edge roughness applied to the airfoil. An increase in the section lift coefficient from 0.20 to

0.80 caused the effectiveness parameter $\left(\frac{\Delta a_0}{\Delta \delta_a} \right)_{\delta_a = \pm 20^\circ}$

to decrease for the true-contour aileron and to increase for the straight-sided and beveled ailerons. The value

of $\left(\frac{\Delta a_0}{\Delta \delta_a} \right)_{\delta_a = \pm 20^\circ}$ for the beveled aileron is question-

able because of a jump in the lift curve at $c_l = 0.80$ and $\delta_a = 20^\circ$ (fig. 16(b)). The aileron effectiveness decreased slightly when the Reynolds number was increased from 1×10^6 to 9×10^6 , as shown in table II and figure 22.

Aileron Hinge Moments

Section characteristics. - The effect of aileron contour on various aileron section hinge-moment parameters is presented in table II. Changes in the aileron contour from the true airfoil contour to straight sides or to a beveled trailing edge increased the values of c_{h_a} and c_{h_b} positively. It is evident from figure 17(b)

that the exact value of c_{h_a} at $\alpha_0 = 0^\circ$ for the beveled aileron is considerably less than 0.0069 as given in table II but, because of the sharp changes in the variation of c_h with α_0 near a section angle of attack of 0° , an average slope was used for c_{h_a} between values of α_0 of -2° and 2° . An increase in the Reynolds number from 1×10^6 to 9×10^6 provided a positive increase in c_{h_a} for all three ailerons and in c_{h_b} for the beveled aileron only (table II). A comparison of the aileron hinge-moment characteristics for a Reynolds number of 9×10^6 (figs. 4, 11, and 17) shows that as the aileron was thickened and beveled near the trailing edge, abrupt changes in c_h occurred in the low angle-of-attack range.

A comparison of figures 17 and 20 shows that the abrupt changes in c_h for the beveled aileron disappear when roughness is applied to the leading edge of the airfoil. The hinge-moment characteristics of a beveled aileron, therefore, may be sensitive to wing-surface roughness.

Data showing the variation of the increments of c_{h_a} and c_{h_b} with changes in trailing-edge angle of various ailerons on some NACA airfoil sections are given in reference 4. When based on the change in trailing-edge angle from the true-airfoil contour, the increments of c_{h_a} and c_{h_b} for the straight-sided and beveled ailerons with the airfoil either smooth or with standard roughness applied to the leading-edge fall within the experimental scatter of the data of reference 4.

The effects of Reynolds number on $\Delta\alpha/q_0$ can be seen in figure 22. An increase in the Reynolds number from 1×10^6 to 9×10^6 decreased the available pressure difference across the aileron seal.

Basis for comparison.— The rate of roll generated by the aileron has an important effect on the hinge moment because the rate of roll alters the mean angle of attack at which the aileron is operating. For comparison of ailerons from section data, therefore, the aileron hinge-moment characteristics are usually determined by use of

the constant-lift concept, that is, the assumption that the aileron portion of the wing acts at constant lift during a steady roll. In reference 1, however, Gates and Irving indicated that the constant-lift concept overstresses the importance of the hinge-moment parameter $c_{h\alpha}$ and gave the equation for the rate of change of the hinge-moment coefficient with aileron deflection in steady roll as

$$c_{h\delta_T} = c_{h\delta} \left(1 - n \frac{c_{h\alpha}}{c_{h\delta}} \right) \quad (3)$$

rather than

$$c_{h\delta_T} = c_{h\delta} \left(1 + \frac{\partial \alpha}{\partial \delta} \frac{c_{h\alpha}}{c_{h\delta}} \right) \quad (4)$$

which is the equation for the constant-lift concept. Although equation (3) is inadequate for computing finite-span characteristics, it is satisfactory for comparing the three ailerons of different contour. In order to simplify the application of equation (3) to nonlinear curves, the equation was converted to Δc_{H_T} by

$$\Delta c_{H_T} = \left(\frac{c_a}{c} \right)^2 \left\{ (\Delta c_h)_\delta \left[1 - \frac{\Delta \alpha_0 / \Delta \delta_a}{(\Delta c_h)_5} \frac{(\Delta c_h)_a}{(\Delta c_h)_5} \right] \right\} \quad (5)$$

A typical value of $1/5$ is given for n in reference 1. The value corresponds to several wing-aileron combinations, one of which is a wing with an aspect ratio of 9 and with a $0.20c$ aileron having an equal up-and-down deflection and extending from 55 percent semispan to the wing tip. The value $n = \frac{1}{5}$ was used in equation (5). The

method of analysis used herein is considered suitable for comparing the relative merits of the three ailerons.

The analysis is presented in the form of the equivalent change in section angle of attack $\Delta \alpha_0$ required to

maintain a constant section lift coefficient for various deflections of the aileron from neutral. The hinge-moment parameter $\frac{\Delta c_{HT}}{\Delta a_0 / \Delta \delta_a}$, which is the ratio of the increment

in hinge-moment coefficient in steady roll (equation (5)) to the aileron effectiveness, is plotted against the equivalent change in angle of attack. The method of analysis takes into account the aileron effectiveness, the hinge moment, and the possible mechanical advantage between the controls and the ailerons. The span of the ailerons and possible effects of three-dimensional flow are not considered except as indicated in equation (5). The smaller the value of the hinge-moment parameter for a given value of Δa_0 , the more advantageous the combination should be for providing a lower control force for a given helix angle of the wing tip $\frac{p_b}{2V}$.

Plain aileron.- In order to compare the plain ailerons of different contour, values of the hinge-moment parameter $\frac{\Delta c_{HT}}{\Delta a_0 / \Delta \delta_a}$ are plotted against Δa_0 in figure 23. Figure 23

indicates that thickening and beveling the trailing edge of the aileron would improve the control-force characteristics of a sealed-gap 0.20c plain aileron. The application of standard roughness to the airfoil causes the hinge-moment parameter to decrease in magnitude for small values of Δa_0 and to increase for large values of Δa_0 .

Balanced aileron.- For comparisons of the three ailerons of different contour with sealed internal balance, the effects of small changes in the pressure difference across the aileron seal and changes in wing roughness are important. For a conservative design, the internally balanced aileron should be so proportioned as to avoid overbalance when the wing has the roughest surface that would be expected in service. For the airfoil with standard leading-edge roughness, the chord of overhang c_b necessary to balance each aileron to $c_{h\delta_T} = -0.001$

was computed by means of the following equations:

$$c_{h\delta_{\text{balance}}} = c_{h\delta_{\text{no balance}}} + \frac{p_b}{2} \left[\left(\frac{c_b}{c_a} \right)^2 - \left(\frac{t/2}{c_a} \right)^2 \right] \quad (6)$$

$$c_{ha_{balance}} = c_{ha_{no\ balance}} + \frac{F_a}{2} \left[\left(\frac{c_b}{c_a} \right)^2 - \left(\frac{t/2}{c_a} \right)^2 \right] \quad (7)$$

$$c_{h\delta_T} = c_{h\delta} \left(1 - \frac{1}{5} \frac{c_{ha}}{c_{h\delta}} \right) \quad (8)$$

The computed overhangs c_b/c_a were 0.536, 0.531, and 0.396, respectively, for the true-contour, straight-sided, and beveled ailerons. The hinge-moment coefficients for the angle-of-attack and aileron-deflection ranges were then calculated from the data on the hinge-moment and seal-pressure-difference coefficients for the plain aileron by use of equations (1) and (2). The approximate limiting deflections of the three sealed internally balanced ailerons of true airfoil contour, straight sides, and a beveled trailing edge were $\pm 15^\circ$, $\pm 15^\circ$, and $\pm 20^\circ$, respectively. The maximum deflections were limited by the lengths of the sealed internal balances.

For comparison of three sealed internally balanced ailerons, values of the hinge-moment parameter

$\frac{\Delta c_{H_T}}{\Delta a_n / \Delta \delta_a}$ are plotted against Δa_n in figure 24.

Figure 24 shows that the straight-sided aileron should provide the smallest control force of the three sealed internally balanced ailerons. The order of merit of the three ailerons changed when the internal balance was added because of the effects of aileron contour on the available seal-pressure-difference coefficient at the higher aileron deflections. For a wing with a smoother surface than that for which the conservative amount of sealed internal balance was determined, the control force for the straight-sided aileron would change the least of the three ailerons. This small change in the control force for the straight-sided aileron can be seen in figure 24 by a comparison of the values of $\frac{\Delta c_{H_T}}{\Delta a_n / \Delta \delta_a}$ for the smooth airfoil with those for the airfoil with standard leading-edge roughness.

Lift

The effects of aileron contour, Reynolds number, and standard airfoil leading-edge roughness on the lift-curve slope c_{l_a} for the NACA 65-210 airfoil section with the aileron neutral are shown in table II. A study of table II shows that c_{l_a} is changed by either roughness or Reynolds number by less than 2 percent regardless of the aileron contour. A reduction in lift-curve slope, however, of approximately 2 and 7 percent, respectively, resulted when the aileron was changed from the true airfoil contour to straight sides or to a beveled trailing edge.

A comparison of figures 3, 10, and 16 shows that for the airfoil with smooth surfaces the maximum section lift coefficient of the NACA 65-210 airfoil section with the aileron neutral was approximately 5 percent less for the model with the straight-sided or beveled ailerons than with the true-contour aileron. This loss in maximum section lift coefficient is attributed to the change in camber over the rear part of the airfoil section caused by the aileron-contour modification. A comparison of figures 7, 13, and 19 shows that, for the airfoil with standard leading-edge roughness, the maximum section lift coefficient was the same for the true-contour and straight-sided ailerons but that the maximum section lift coefficient for the beveled aileron was less than that for the true-contour aileron.

Pitching Moment

The effect of aileron contour on the airfoil section pitching moment is shown in table II and figure 22. The rate of change of $c_{m_c}/4$ with c_l becomes less negative, which corresponds to a forward shift in the aerodynamic center, as the aileron contour is changed from the true airfoil contour to straight sides or to a beveled trailing edge. This change in aerodynamic center agrees with the results of references 5 and 6. An increase in the Reynolds number from 1×10^6 to 9×10^6 had no appreciable effect on the variation of $c_{m_c}/4$ with c_l at a constant section lift coefficient of 0.20¹⁴ (fig. 22).

Because the changes in section pitching moment of an airfoil induced by aileron deflection are of primary importance in determining the lateral-control reversal speed, the variation of the increment in section pitching-moment coefficient $\Delta c_{m_c}/4$ with the equivalent change in section angle of attack required to maintain a constant section lift coefficient was plotted for the three ailerons (fig. 25). The variation of $\Delta c_{m_c}/4$ with Δa_o was approximately the same for the three ailerons tested (fig. 25). The rate of change of $\Delta c_{m_c}/4$ with Δa_o is 0.0205, which agrees with the theoretical and experimental values given in reference 7.

Drag

The effect of aileron contour on the airfoil section profile-drag coefficient is presented in figure 26. With the aileron neutral, changes in the aileron contour within the range investigated show no significant effect on the airfoil section profile-drag characteristics.

The variation of airfoil section profile-drag coefficient c_{d_o} with section angle of attack a_o for various aileron deflections is presented in figure 6 for the true-contour aileron at Reynolds numbers of 1×10^6 and 9×10^6 . At a Reynolds number of 9×10^6 , a low-drag "bucket" was realized at all aileron deflections (fig. 6). Because the change in c_{d_o} with aileron contour was small with the aileron neutral, the section profile-drag characteristics of the airfoil with either the straight-sided or beveled aileron deflected would probably be the same as for the airfoil with the true-contour aileron.

CONCLUSIONS

A two-dimensional wind-tunnel investigation was made of an NACA 65₁-210 airfoil equipped with three interchangeable sealed-gap 0.20-airfoil-chord plain ailerons of different contour. The airfoil was tested with smooth surfaces and with standard leading-edge roughness. The data obtained indicated the following conclusions:

1. Changing the aileron contour by thickening or beveling the trailing edge would cause

- (a) The aileron section effectiveness parameter a_5 to decrease
 - (b) The rate of change of aileron section hinge-moment coefficient c_h with both section angle of attack α_0 and aileron deflection δ_a to increase positively
 - (c) The rate of change of section lift coefficient c_l with section angle of attack α_0 to decrease
 - (d) The maximum section lift coefficient to decrease
 - (e) The aerodynamic center to shift forward
 - (f) The increment of section pitching-moment coefficient induced by aileron deflection at constant lift to remain the same
 - (g) The section profile-drag coefficient with the aileron neutral to remain substantially unaffected throughout the section angle-of-attack range
2. The application of roughness to the leading edge of the airfoil would accentuate the balancing action of the aileron and the loss in aileron effectiveness caused by beveling the aileron trailing edge.
3. The effect of aileron contour on the hinge moments of sealed internally balanced ailerons, as computed from data on the hinge-moment and seal-pressure-difference coefficients of plain ailerons, showed an appreciable effect of aileron contour on the hinge moments at large aileron deflections even though all three ailerons were computed to have the same hinge-moment slope at small deflections.

Langley Memorial Aeronautical Laboratory
National Advisory Committee for Aeronautics
Langley Field, Va.

REFERENCES

1. Gates, S. B., and Irving, H. B.: An Analysis of Aileron Performance. 4652, S. & C. 1154, Rep. No. B.A. 1624, British R.A.E., July 1940.
2. Abbott, Ira H., von Doenhoff, Albert E., and Stivers, Louis S., Jr.: Summary of Airfoil Data. NACA ACR No. L5C05, 1945.
3. Ames, Milton B., Jr., and Sears, Richard I.: Determination of Control-Surface Characteristics from NACA Plain-Flap and Tab Data. NACA Rep. No. 721, 1941.
4. Purser, Paul E., and Gillis, Clarence L.: Preliminary Correlation of the Effects of Beveled Trailing Edges on the Hinge-Moment Characteristics of Control Surfaces. NACA CB No. 3E14, 1943.
5. Crane, Robert W., and Holtzclaw, Ralph W.: Wind-Tunnel Investigation of Ailerons on a Low-Drag Airfoil. I - The Effect of Aileron Profile. NACA ACR No. 4A14, 1944.
6. Purser, Paul E., and Johnson, Harold S.: Effects of Trailing-Edge Modifications on Pitching-Moment Characteristics of Airfoils. NACA CB No. L4T30, 1944.
7. Purser, Paul E., and McKinney, Elizabeth G.: Comparison of Pitching Moments Produced by Plain Flaps and by Spoilers and Some Aerodynamic Characteristics of an NACA 23012 Airfoil with Various Types of Aileron. NACA ACR No. L5C24a, 1945.

TABLE I
ORDINATES FOR NACA 65₁-210 AIRFOIL SECTION

[Stations and ordinates given in percent of airfoil chord]

Upper surface		Lower surface	
Station	Ordinate	Station	Ordinate
0	0	0	0
.435	.819	.565	-.719
.678	.999	.822	-.859
1.169	1.273	1.331	-.1.059
2.408	1.757	2.592	-.1.385
4.898	2.491	5.102	-.1.859
7.394	3.069	7.606	-.2.221
9.894	3.555	10.106	-.2.521
14.899	4.338	15.101	-.2.992
19.909	4.938	20.091	-.3.346
24.921	5.397	25.079	-.3.607
29.936	5.732	30.064	-.3.788
34.951	5.954	35.049	-.3.894
39.968	6.067	40.032	-.3.925
44.984	6.058	45.016	-.3.868
50.000	5.915	50.000	-.3.709
55.014	5.625	54.986	-.3.435
60.027	5.217	59.973	-.3.075
65.036	4.712	64.964	-.2.652
70.043	4.128	69.957	-.2.184
75.045	3.479	74.955	-.1.689
80.044	2.783	79.956	-.1.191
85.038	2.057	84.962	-.711
90.028	1.327	89.972	-.293
95.014	.622	94.986	.010
100.000	0	100.000	0

L.E. radius: 0.687
 Slope of radius through L.E.: 0.08425

TABLE II.- SECTION PARAMETERS MEASURED AT $\alpha_0 = 0^\circ$ AND $\delta_a = 0^\circ$

EXCEPT FOR $\left(\frac{\Delta\alpha_0}{\Delta\delta_a}\right)_{\delta_a=\pm 20^\circ}$ MEASURED AT $c_l = 0.20$ AND $c_l = 0.80$

Surface	R	c_{l_a}	c_{l_δ}	a_δ	$\left(\frac{\Delta\alpha_0}{\Delta\delta_a}\right)_{\delta_a=\pm 20^\circ}$	$\left(\frac{\Delta\alpha_0}{\Delta\delta_a}\right)_{\delta_a=\pm 20^\circ}$	c_{h_a}	c_{h_δ}	P_a	P_δ	c_{m_a}	c_{m_δ}
(1)					(2)	(3)						
True-contour aileron												
Smooth	9×10^6	0.108	0.052	-0.472	-0.455	-0.449	-0.0066	-0.0136	0.025	0.075	-0.0017	-0.0100
Rough	9×10^6	.107	.049	-.450	-.428	-----	-.0062	-.0122	.024	.075	-----	-----
Smooth	1×10^6	.106	.053	-.490	-.480	-----	-.0092	-.0134	-----	-----	-.0008	-.0100
Straight-sided aileron												
Smooth	9×10^6	0.106	0.050	-0.465	-0.465	-0.480	-0.0050	-0.0112	0.029	0.074	-0.0007	-0.0094
Rough	9×10^6	.105	.047	-.450	-.435	-----	-.0040	-.0110	.025	.074	-----	-----
Smooth	1×10^6	.105	.051	-.485	-.480	-----	-.0071	-.0113	-----	-----	-.0002	-.0104
Beveled aileron												
Smooth	9×10^6	0.100	0.046	-0.460	-0.459	-0.470	0.0069	-0.0070	0.026	0.079	0.0010	-0.0086
Rough	9×10^6	.100	.042	-.415	-.400	-----	.0019	-.0059	.024	.077	-----	-----
Smooth	1×10^6	.099	.047	-.475	-.454	-----	-.0027	-.0100	-----	-----	-.0001	-.0098

¹"Smooth" and "Rough" refer to the airfoil with aerodynamically smooth surfaces and with standard leading-edge roughness.

² $c_l = 0.20$.

³ $c_l = 0.80$.

NACA ACR No. L5F27

Fig. 1

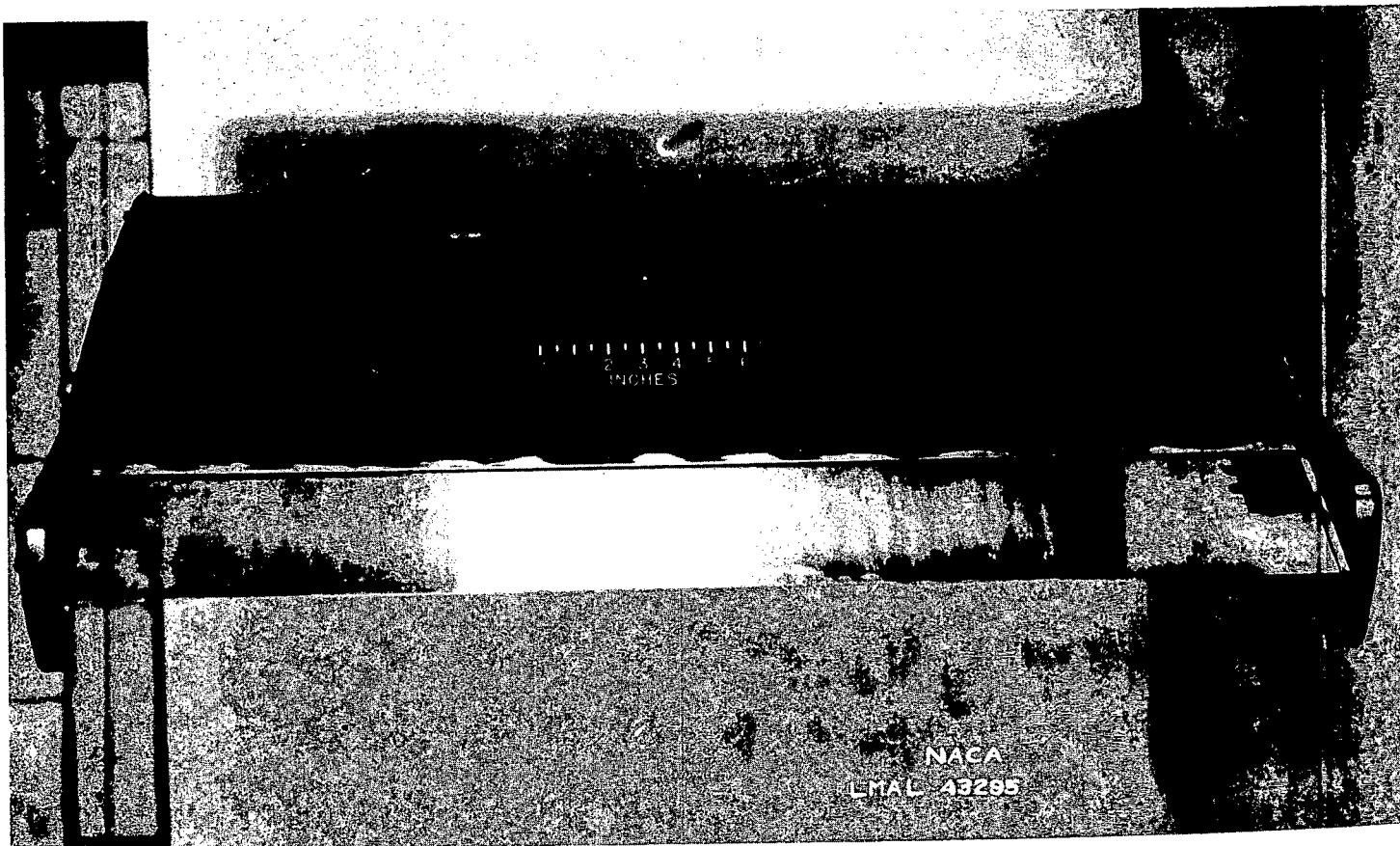
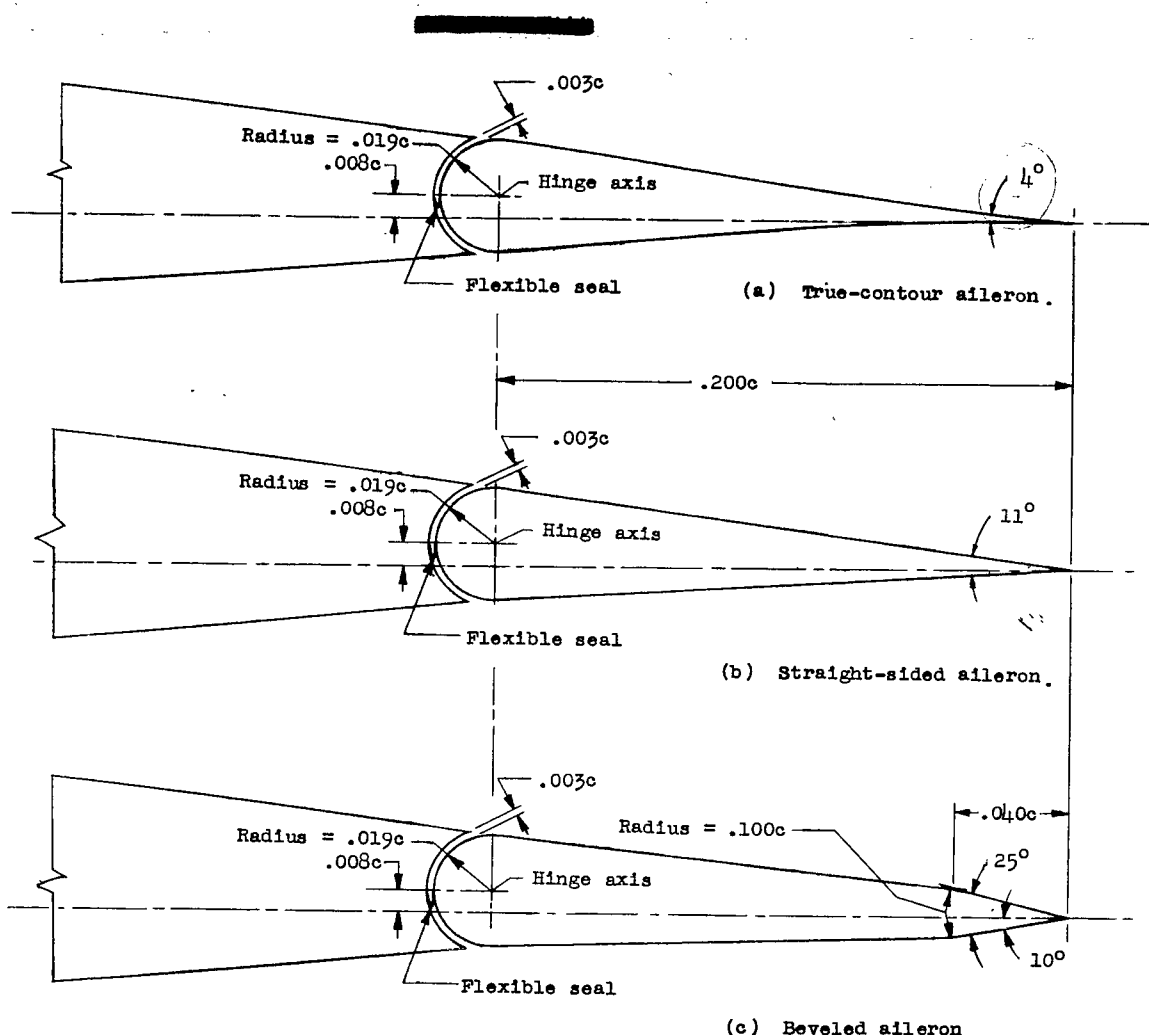


Figure 1.- NACA 65₁-210 airfoil section with aileron, as tested in the
Langley two-dimensional low-turbulence pressure tunnel.



NATIONAL ADVISORY
COMMITTEE FOR AERONAUTICS

Figure 2 .- Sketch of the three sealed-gap plain ailerons on the
NACA 65-210 airfoil section.

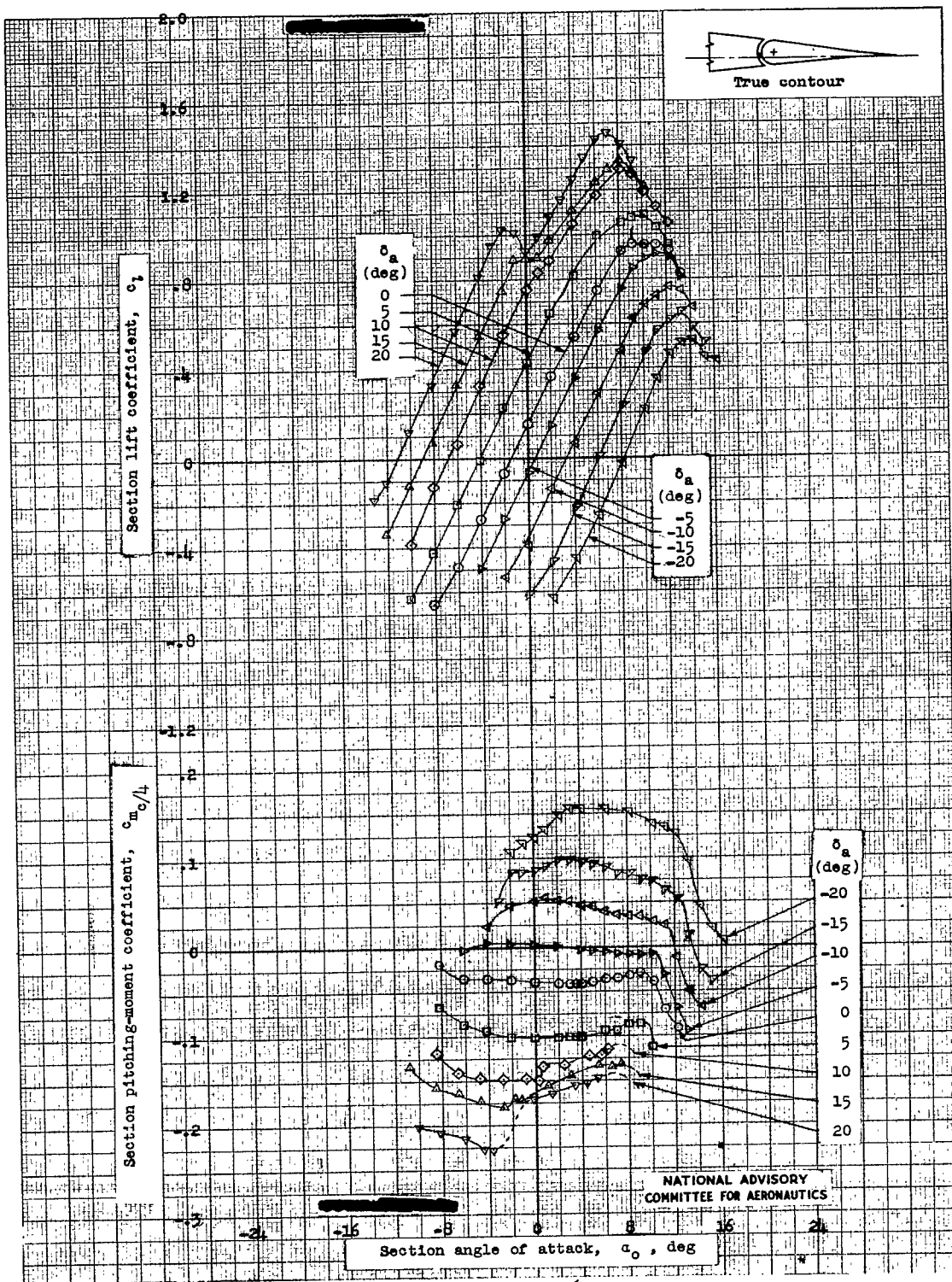
(a) $R = 1 \times 10^6$.

Figure 3 .- Lift and pitching-moment characteristics of an NACA 65₁-210 airfoil section equipped with a sealed-gap 0.20c plain aileron of true airfoil contour. Tests, TDT 847, 849, and 850.

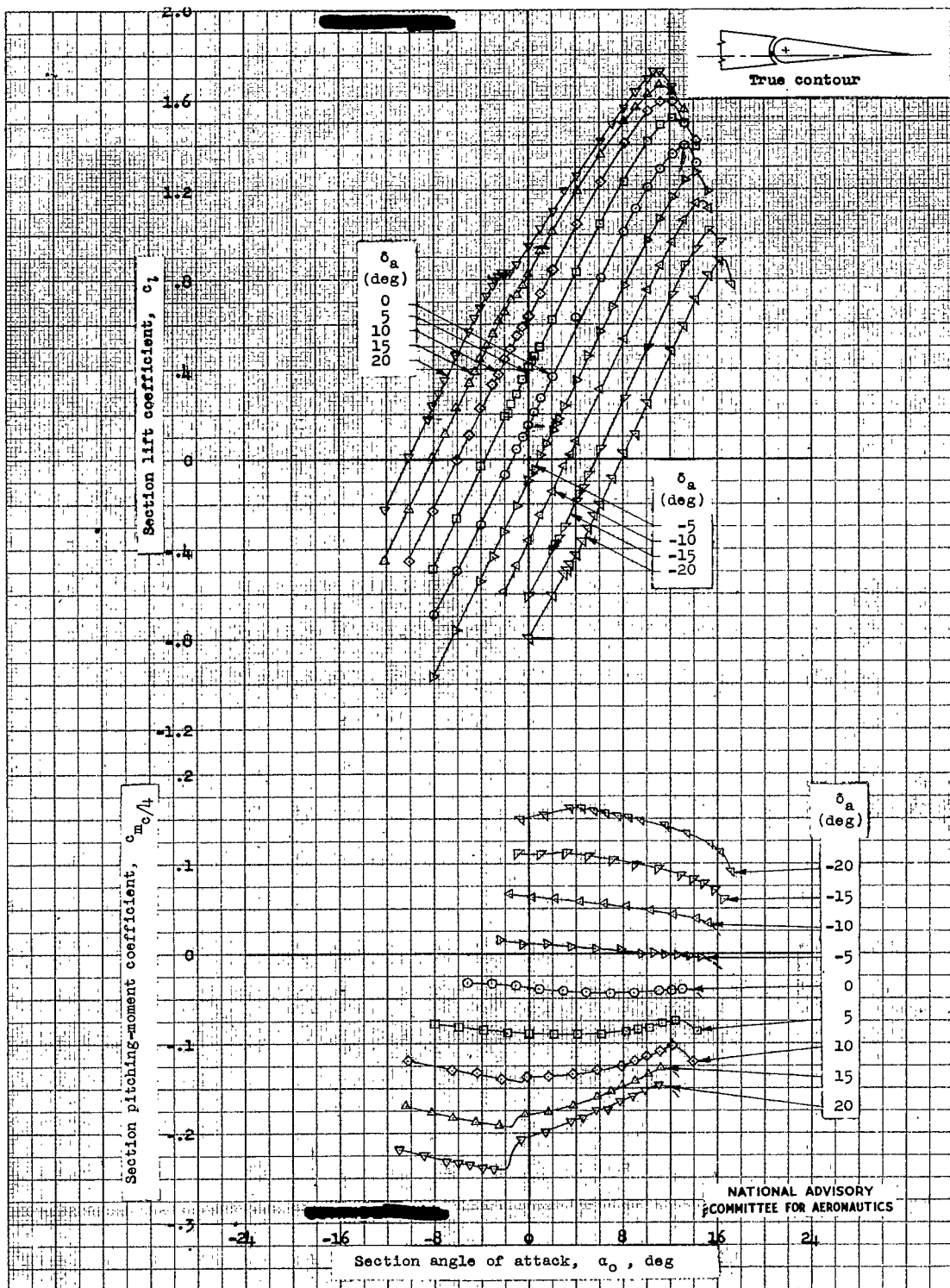
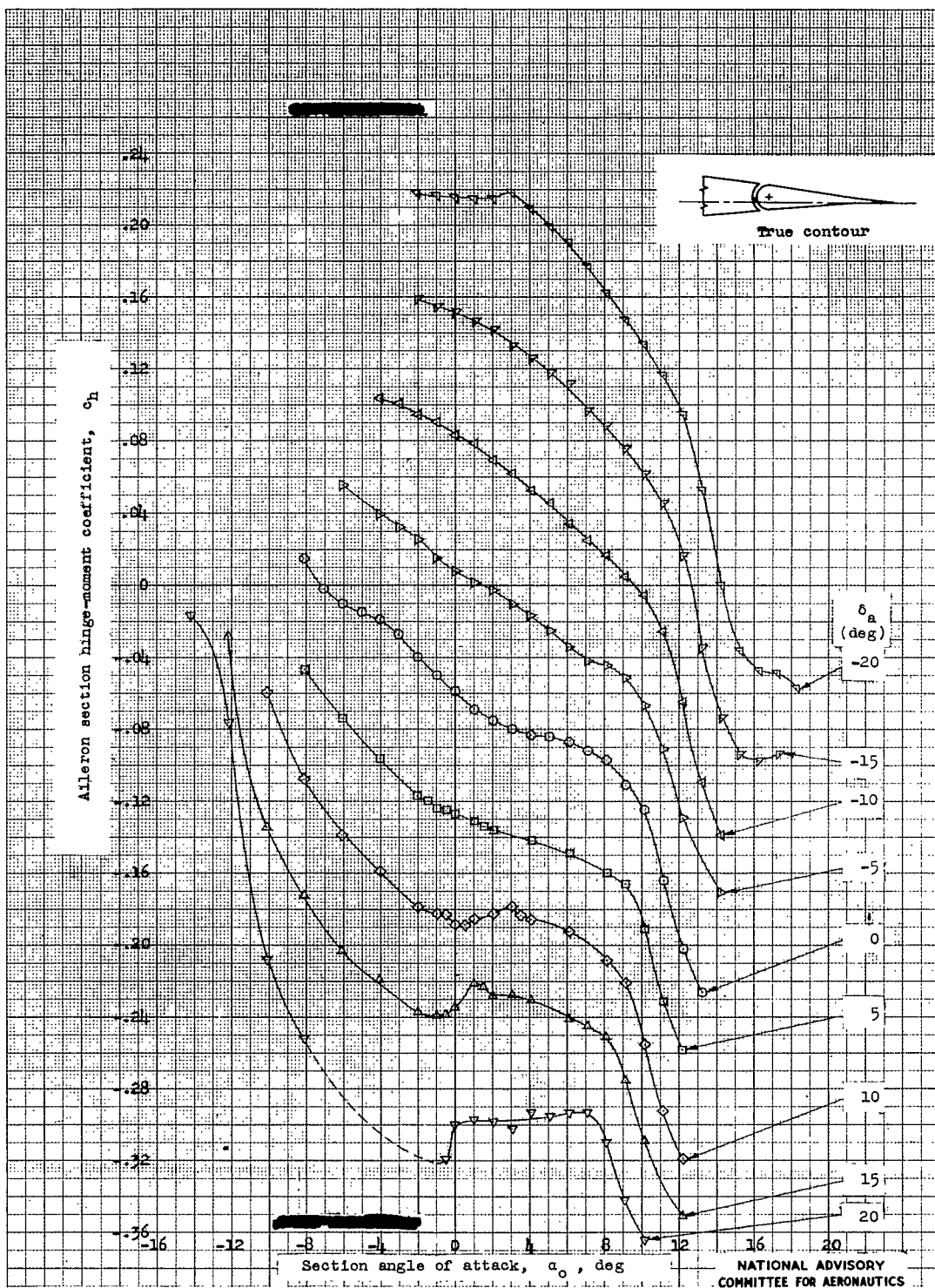
(b) $R = 9 \times 10^6$.

Figure 3 .- Concluded.



(a) $R = 1 \times 10^6$.
Figure 4. - Hinge-moment characteristics of a sealed-gap 0.20c plain aileron of true airfoil contour on an NACA 65₁-210 airfoil section. Tests, IDT 847, 853.

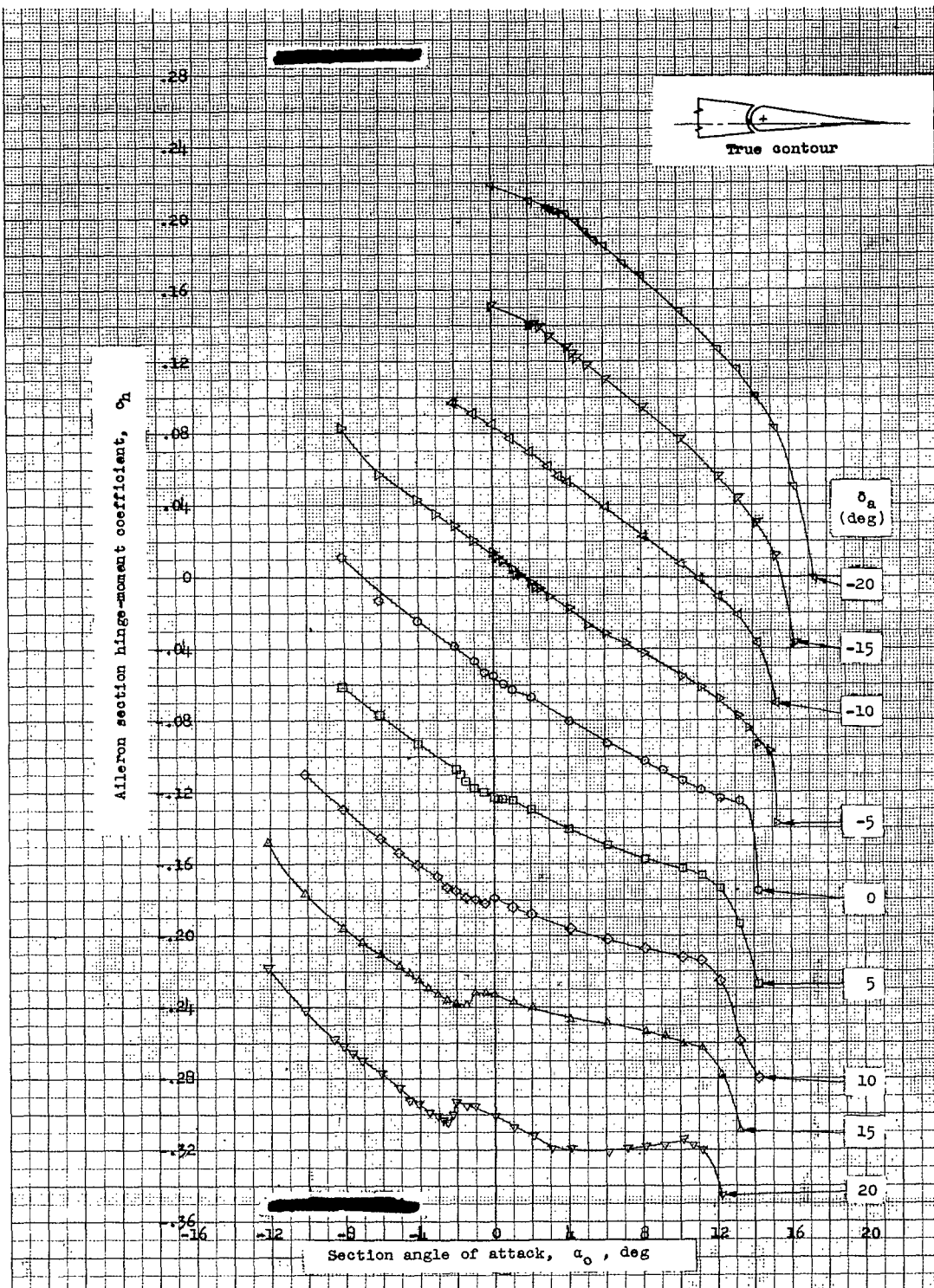
(b) $R = 9 \times 10^6$.NATIONAL ADVISORY
COMMITTEE FOR AERONAUTICS

Figure 4 .- Concluded.

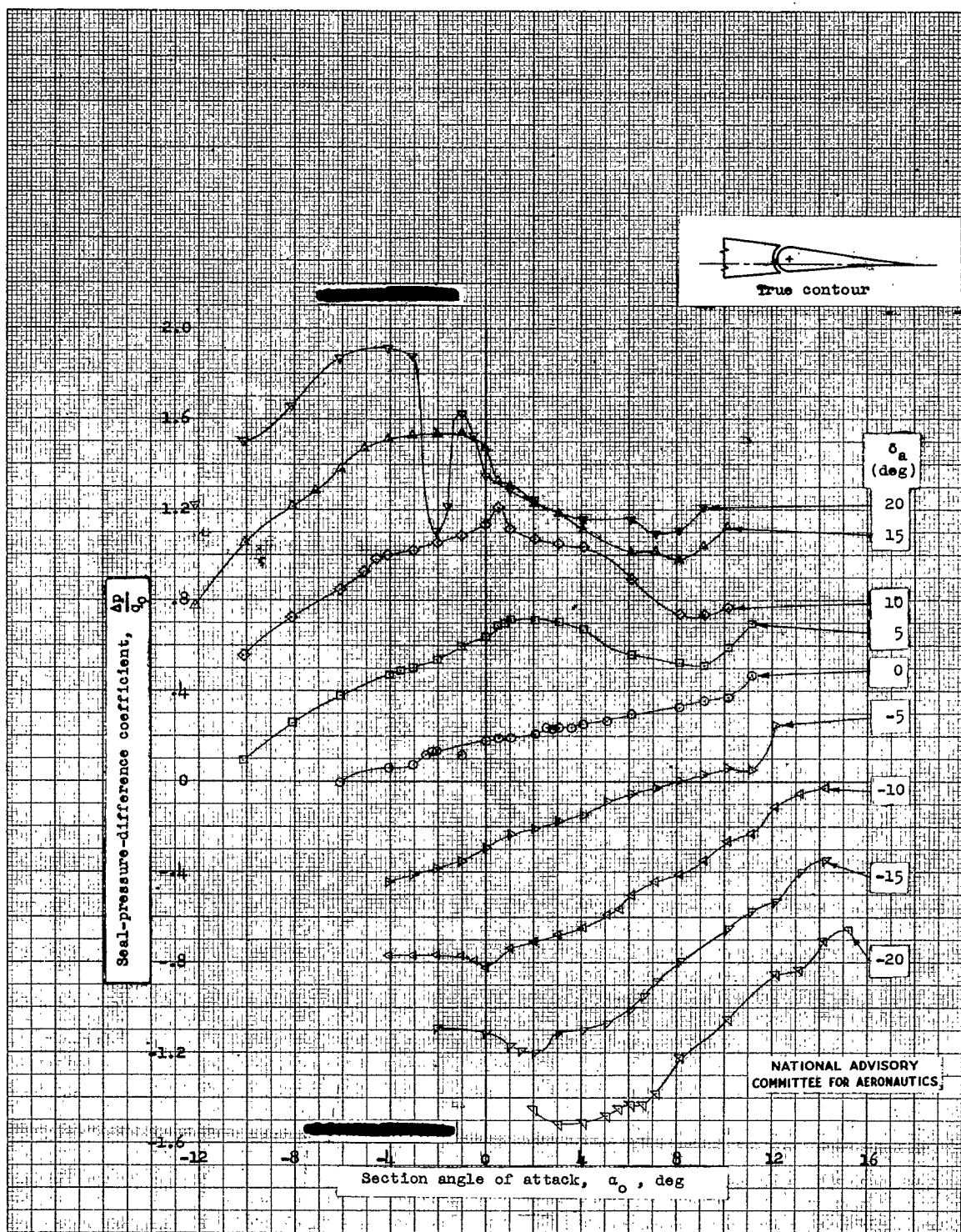
(a) $R = 1 \times 10^6$.

Figure 5... Pressure difference across the gap seal of a 0.20c plain aileron of true airfoil contour on an NACA 65₁-210 airfoil section. Tests, IDT 847 and 848.

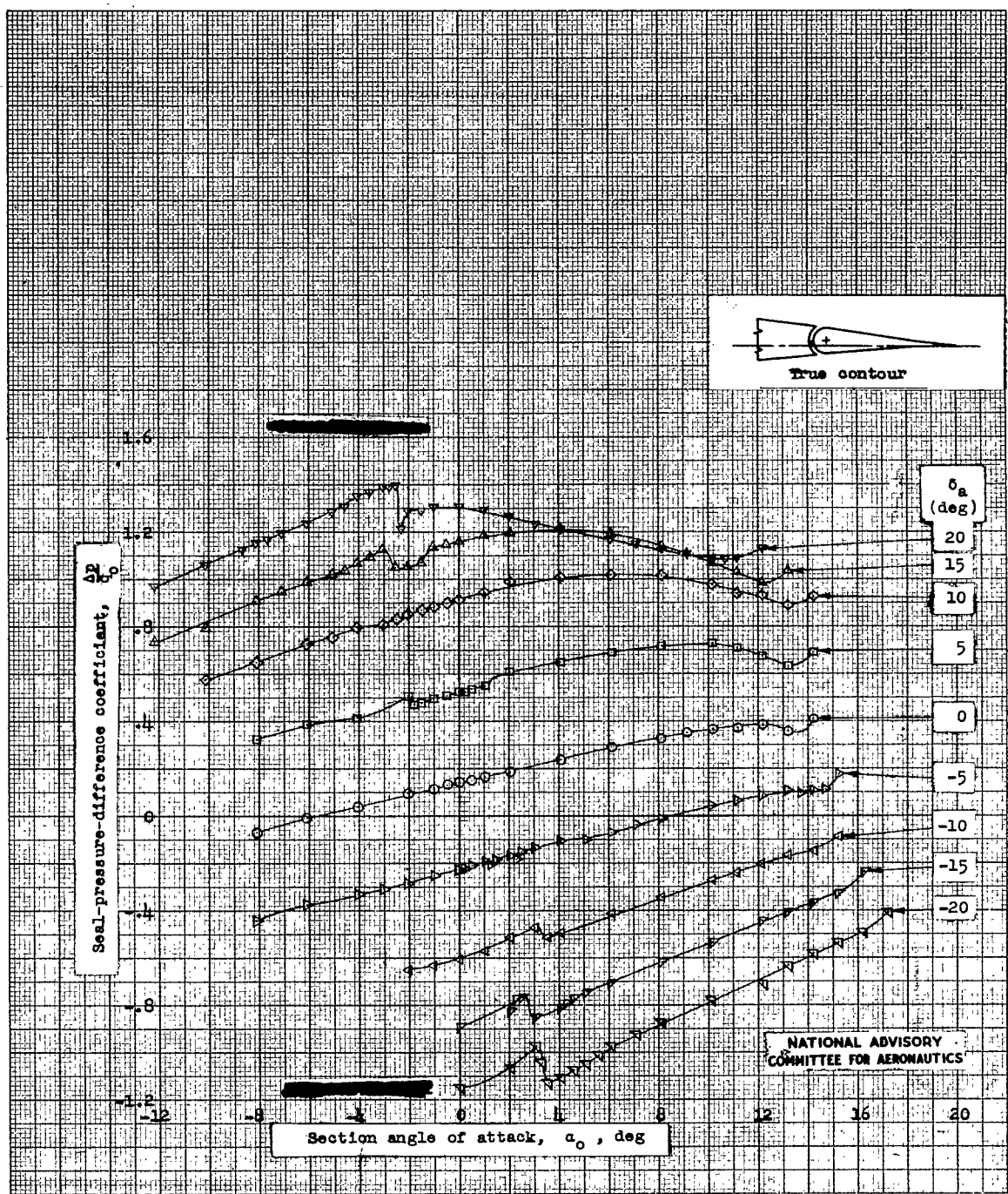
(b) $R = 9 \times 10^6$.

Figure 5 .- Concluded.

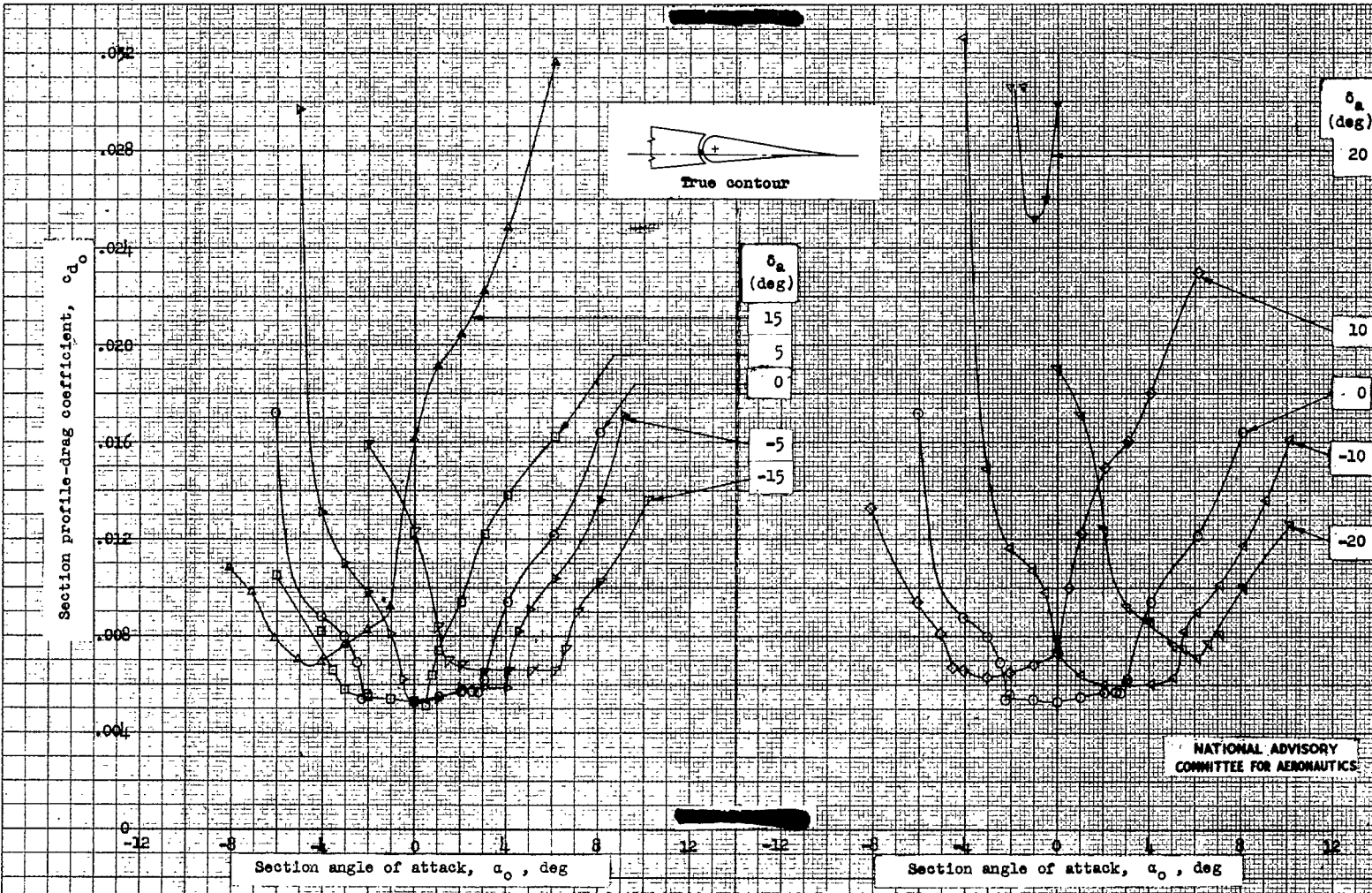
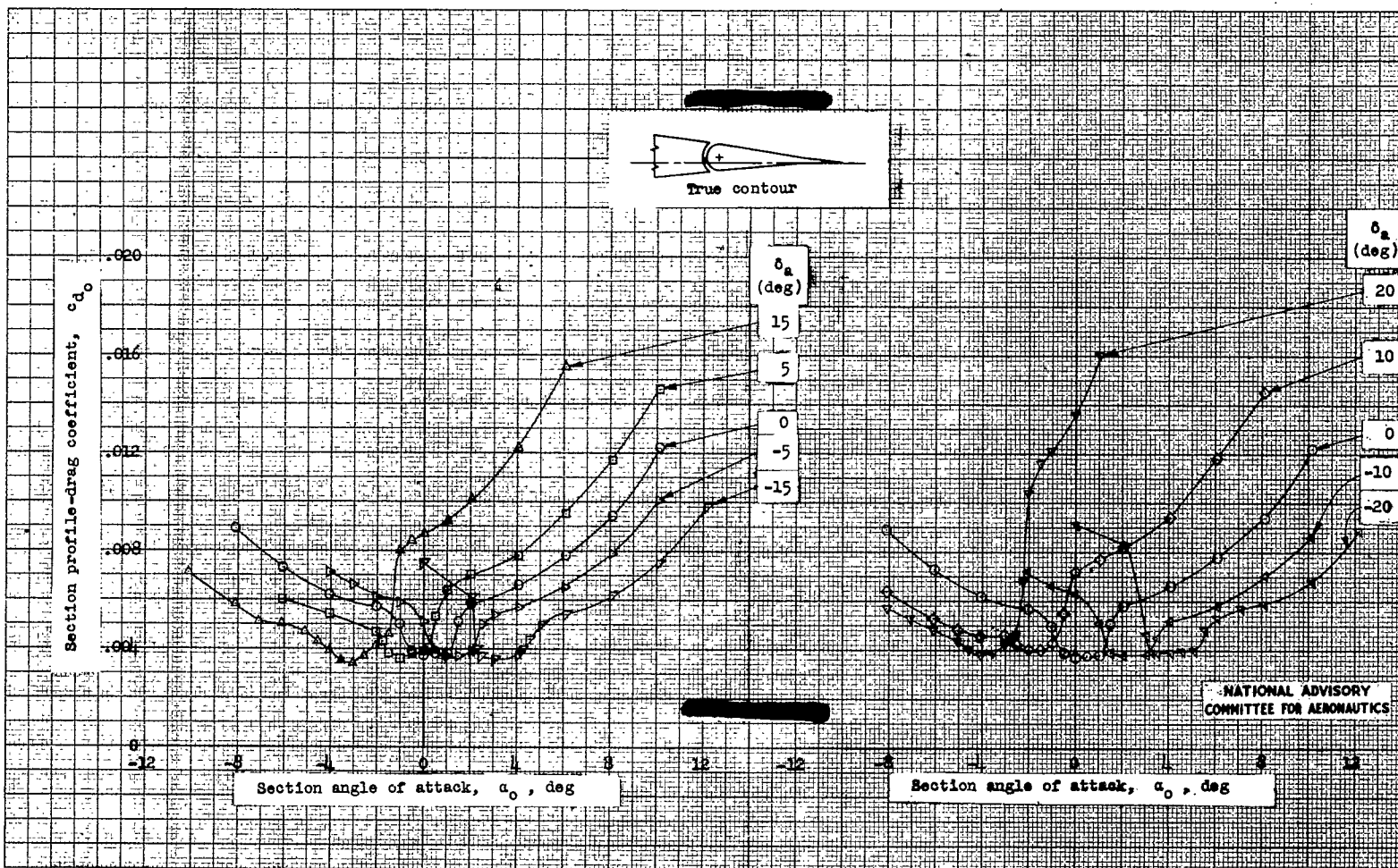
(a) $R = 1 \times 10^6$.

Figure 6 .- Drag characteristics of an NACA 65-210 airfoil section equipped with a sealed-gap 0.20c plain aileron of true airfoil contour. Tests, TDT 845, 847, and 848.



(b) $R = 9 \times 10^6$.

Figure 6 .- Concluded.

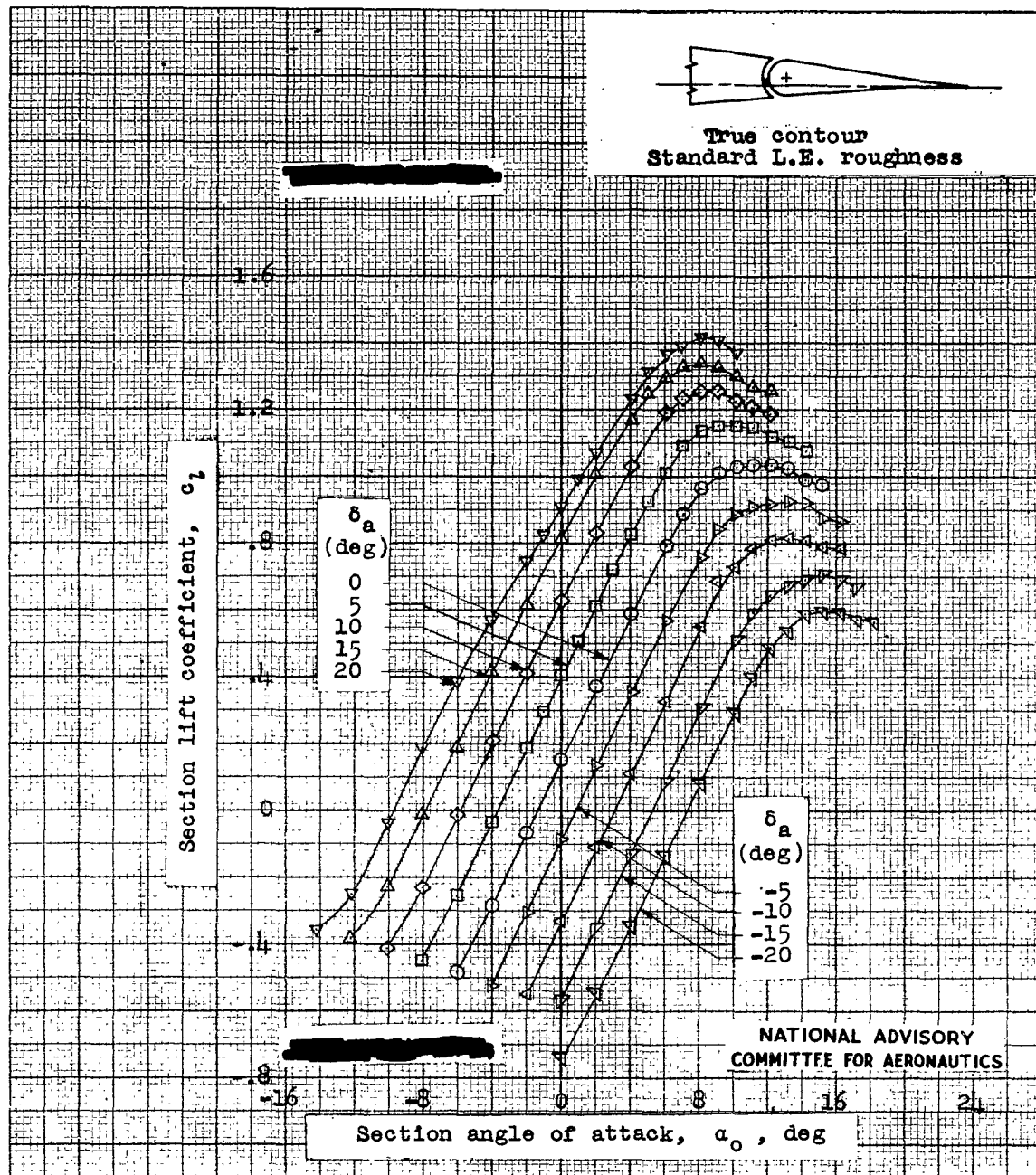


Figure 7.- Lift characteristics of an NACA 65₁-210 airfoil section equipped with a sealed-gap 0.20c plain aileron of true airfoil contour. Standard leading-edge roughness; $R = 9 \times 10^6$; test, IDT 869.

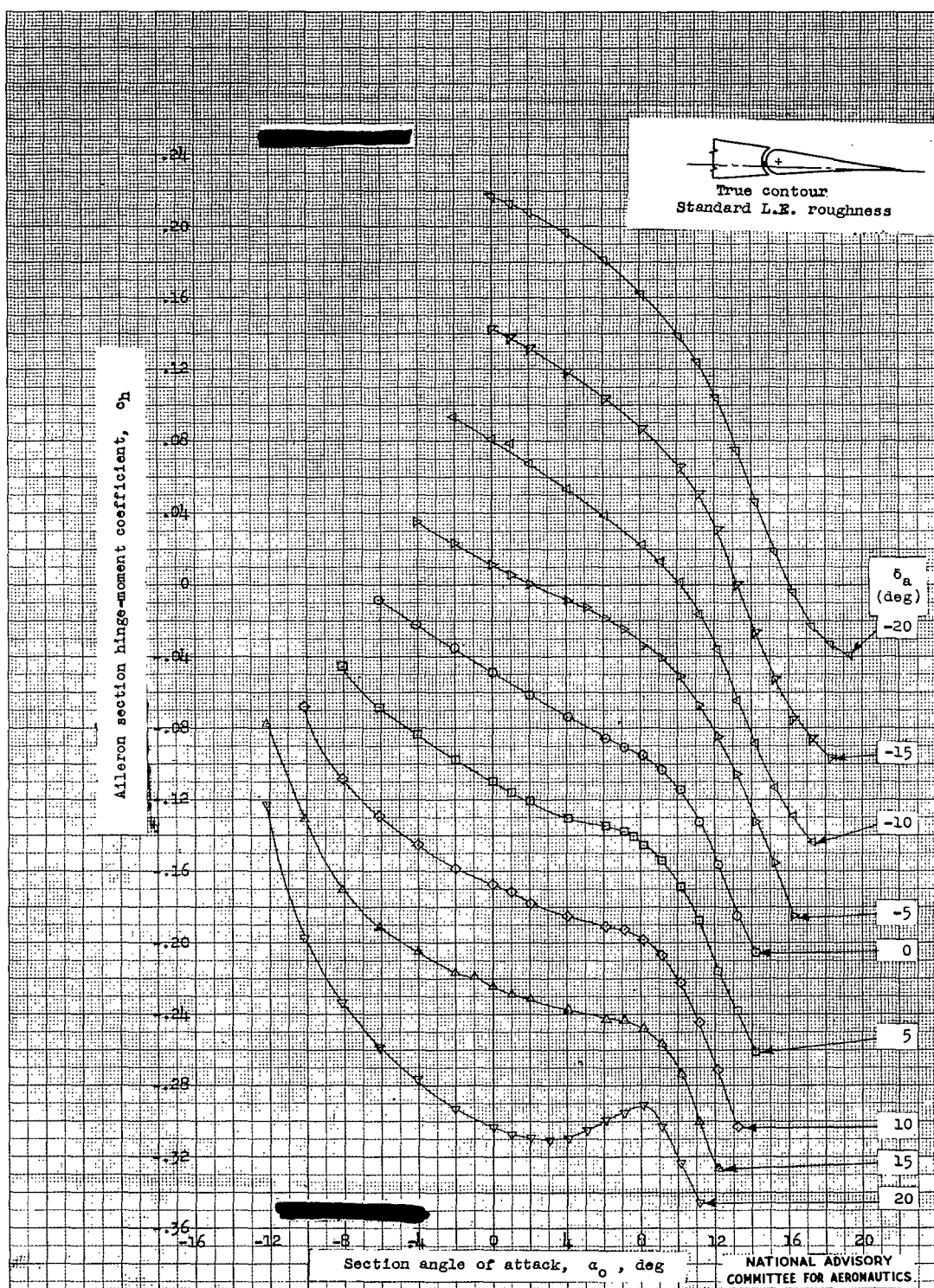


Figure 8.- Hinge-moment characteristics of a sealed-gap 0.20c plain aileron of true airfoil contour on an NACA 65₁-210 airfoil section having standard leading-edge roughness. $R = 9 \times 10^6$; test, TDT 868.

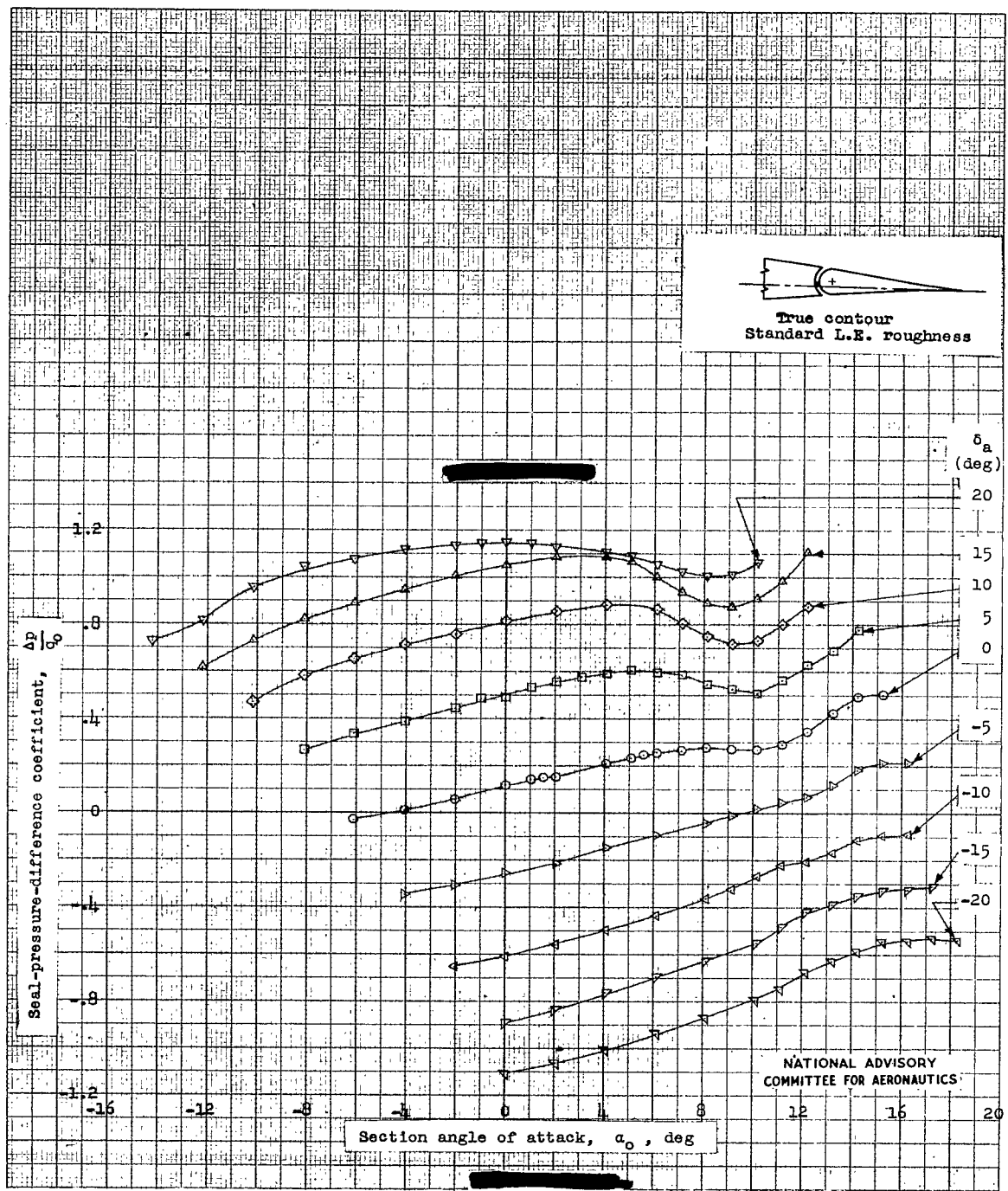


Figure 9.- Pressure difference across the gap seal of a 0.20c plain aileron of true airfoil contour on an NACA 65₁-210 airfoil section having standard leading-edge roughness. $R = 9 \times 10^6$; test, TDT 869.

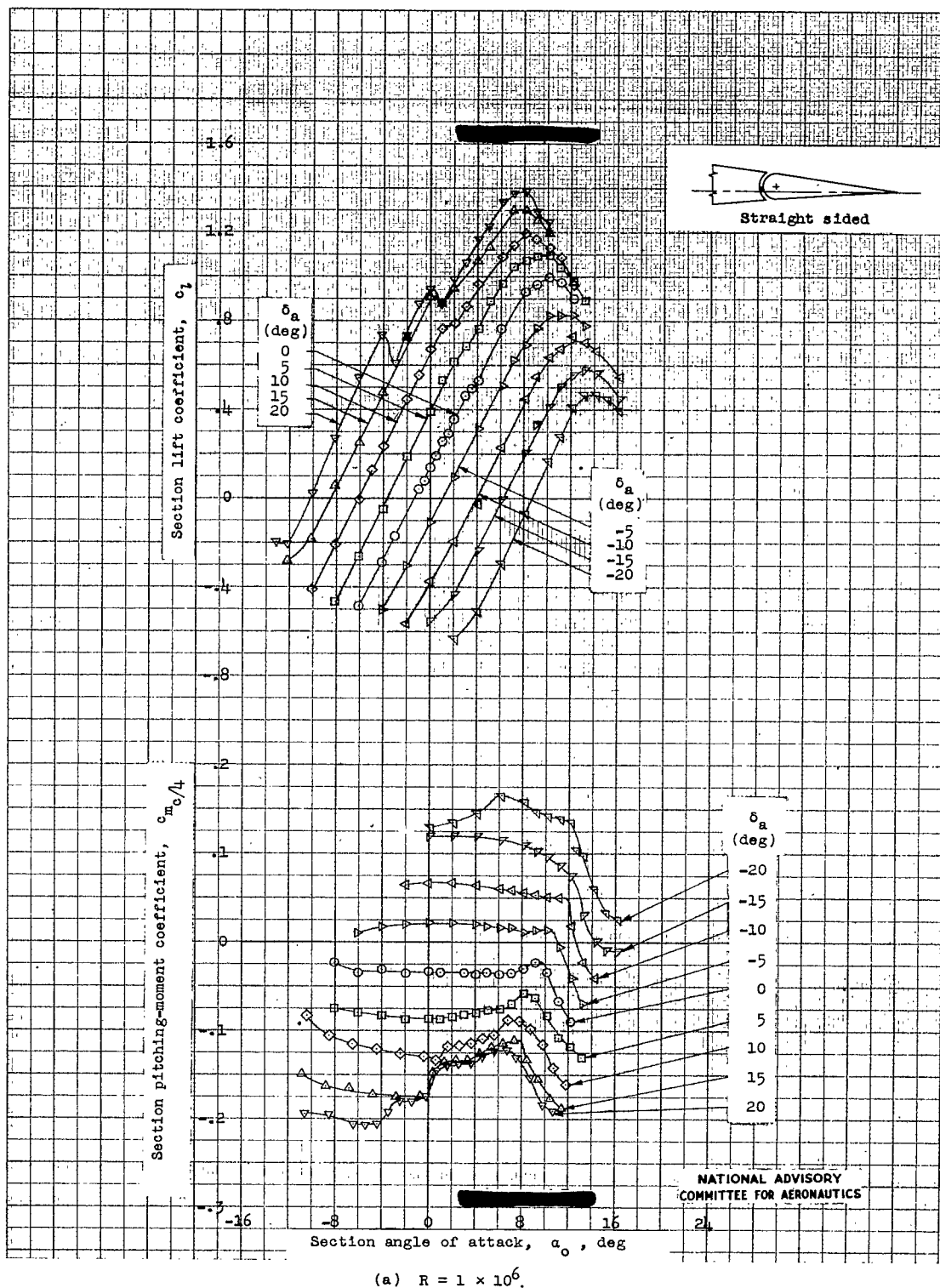
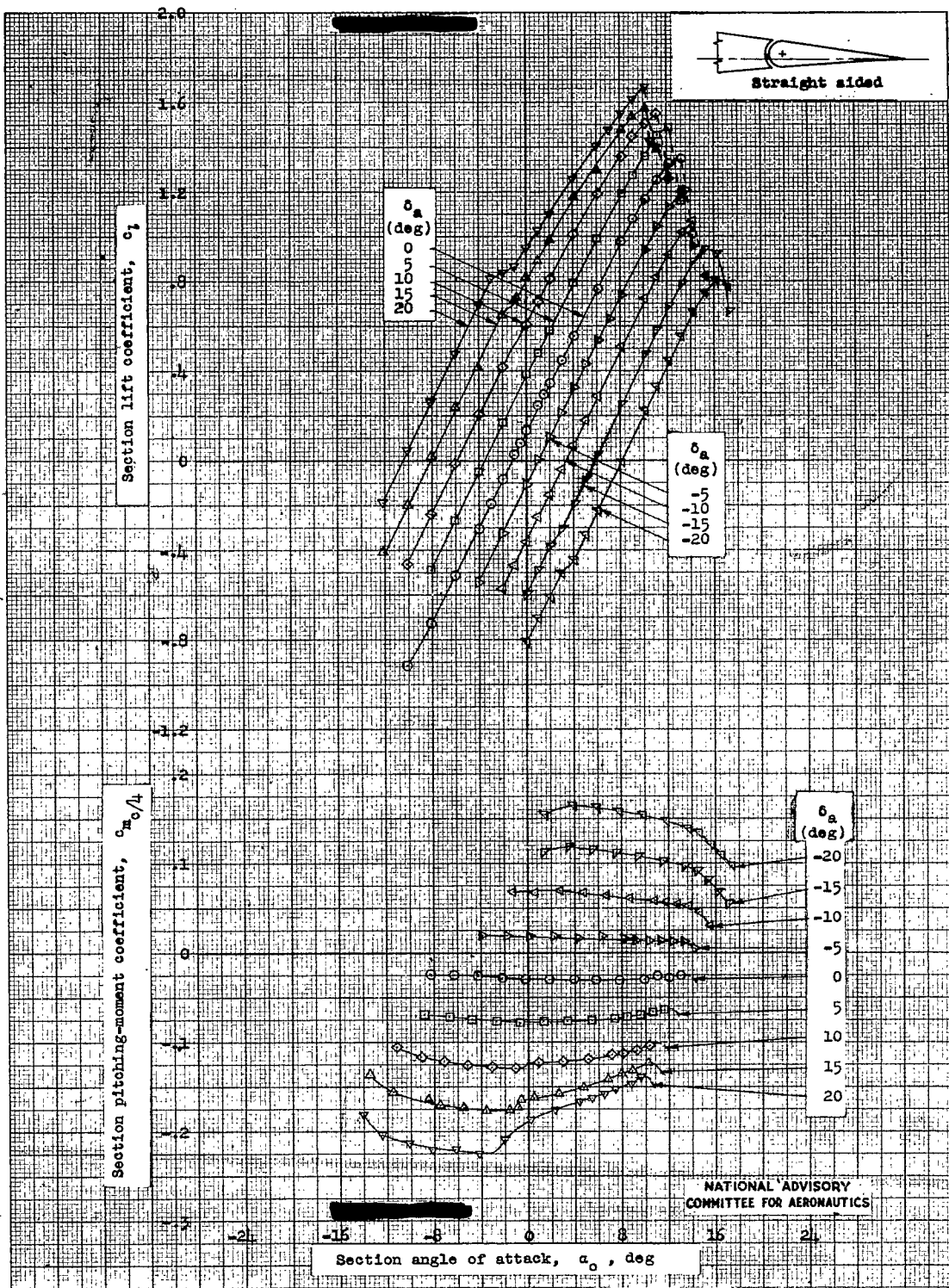


Figure 10.- Lift and pitching-moment characteristics of an NACA 651-210 airfoil section equipped with a sealed-gap 0.20c plain aileron with straight sides. Tests, TDT 854, 861.

(b) $R = 9 \times 10^6$.
Figure 10.- Concluded.

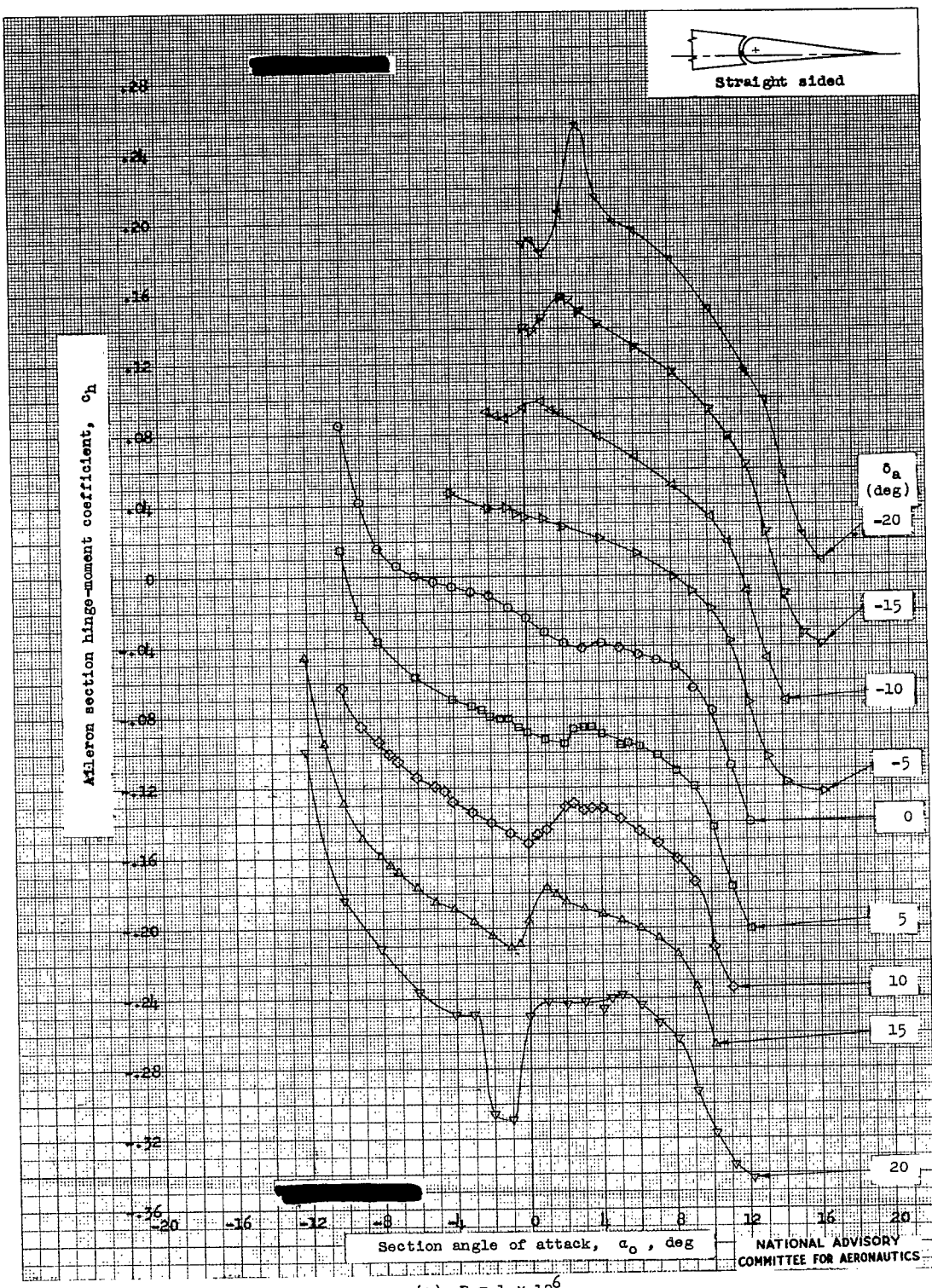
(a) $R = 1 \times 10^6$.

Figure 11.- Hinge-moment characteristics of a sealed-gap 0.20c plain aileron with straight sides on an NACA 651-210 airfoil section. Tests, IDT 852 and 860.

NATIONAL ADVISORY
COMMITTEE FOR AERONAUTICS

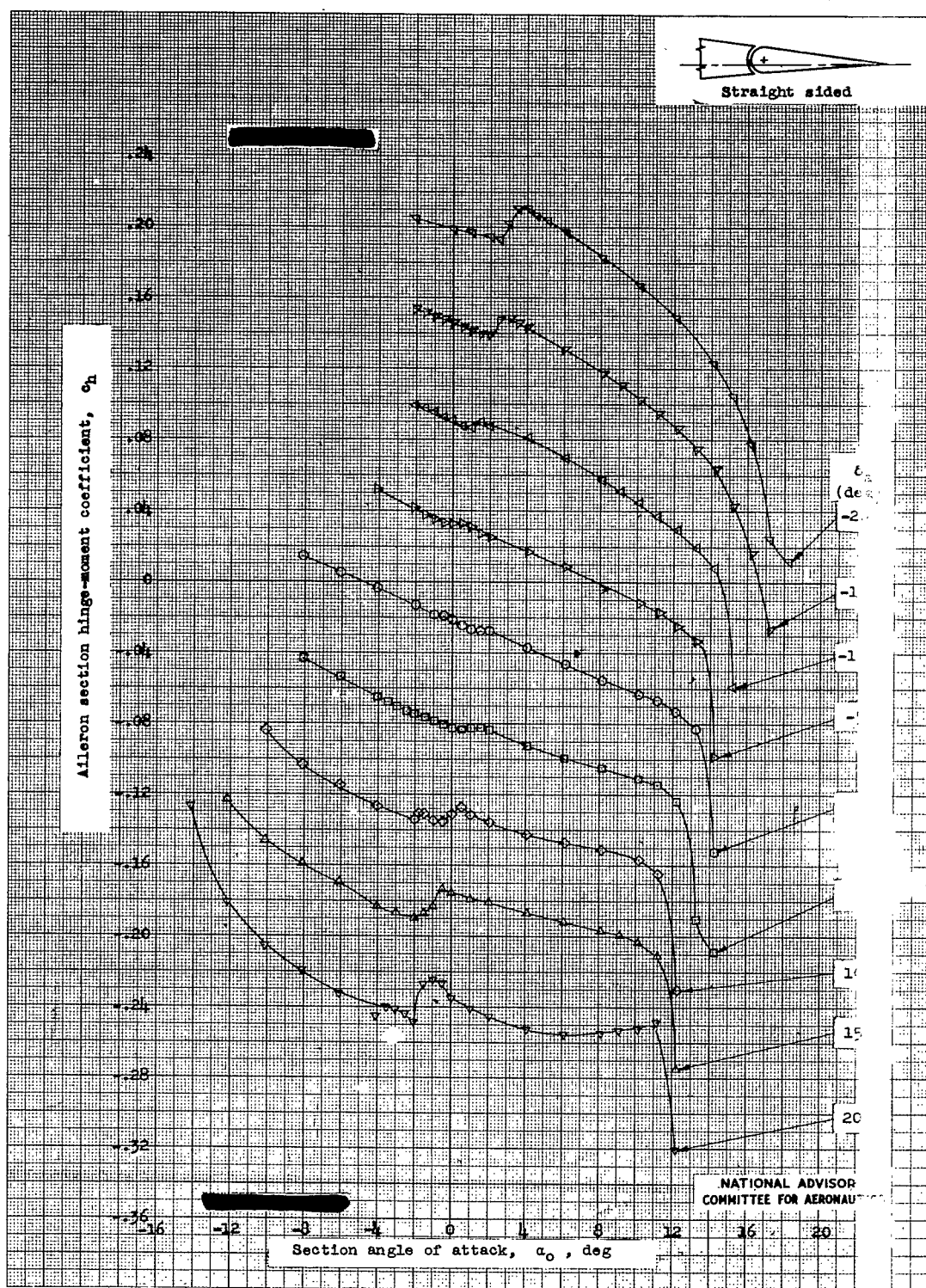


Figure 11.. Concluded.

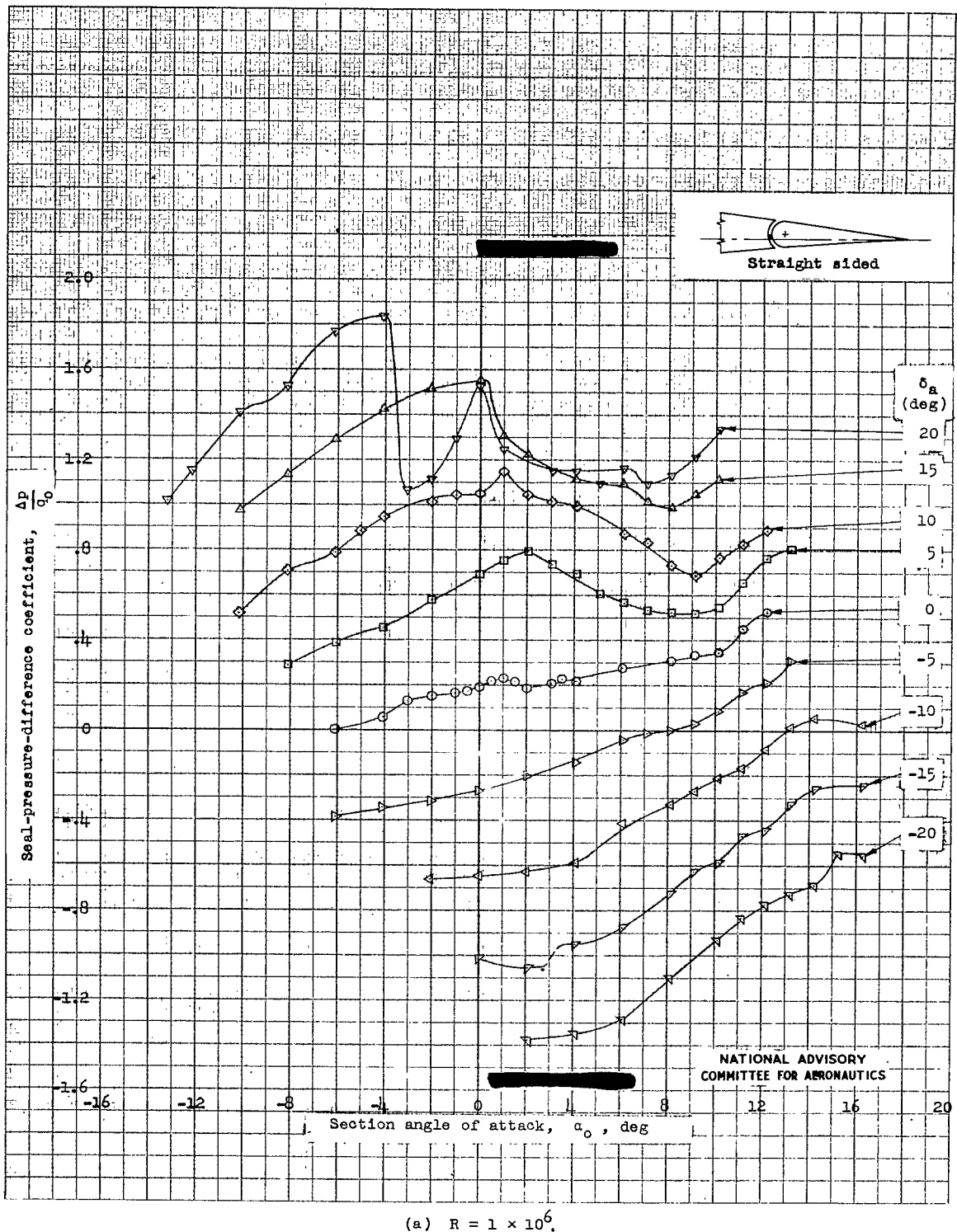
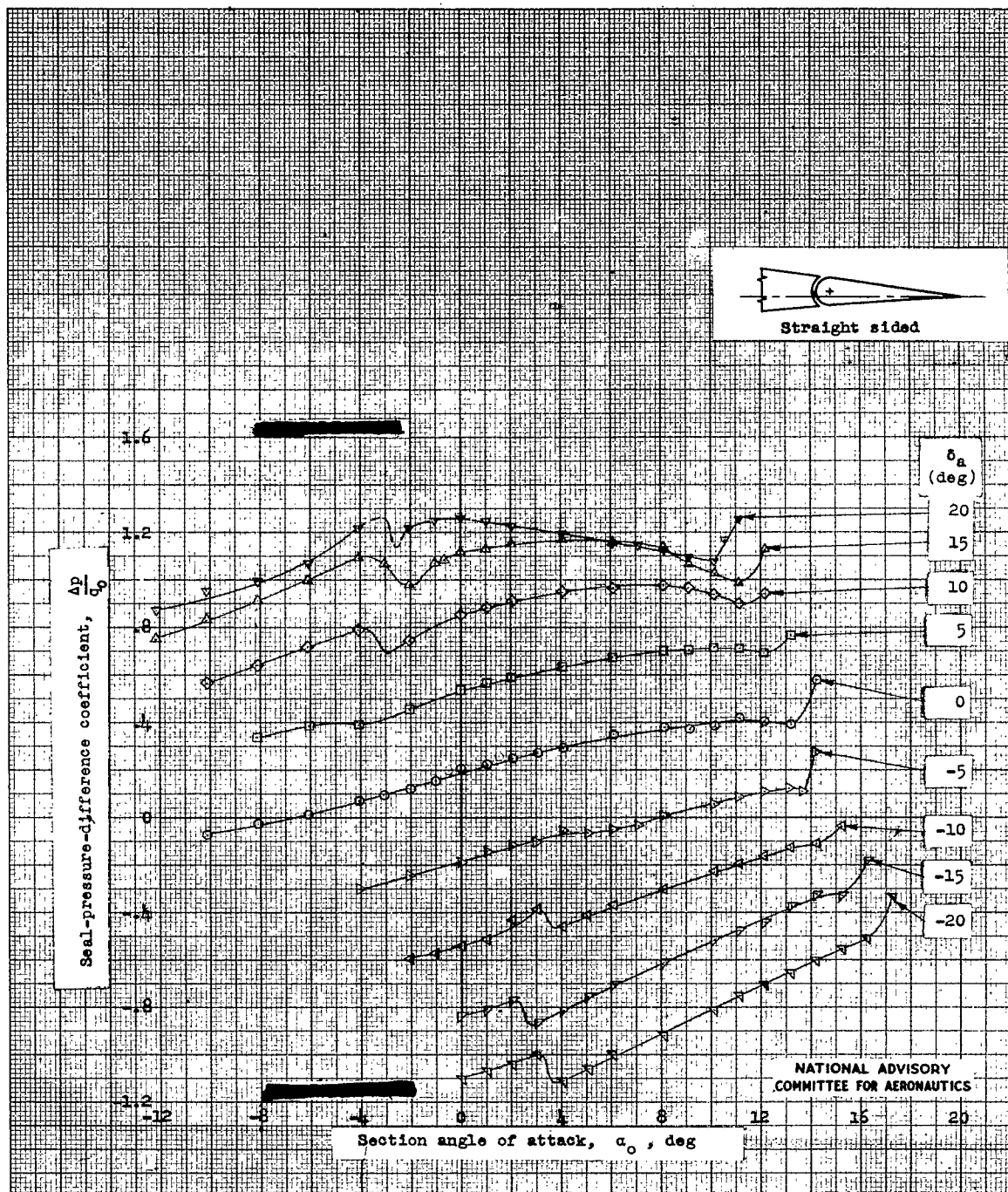


Figure 12.- Pressure difference across the gap seal of a 0.20c plain aileron with straight sides on an NACA 65₁-210 airfoil section. Test, TDT 854.



(b) $R = 9 \times 10^6$.
Figure 12.- Concluded.

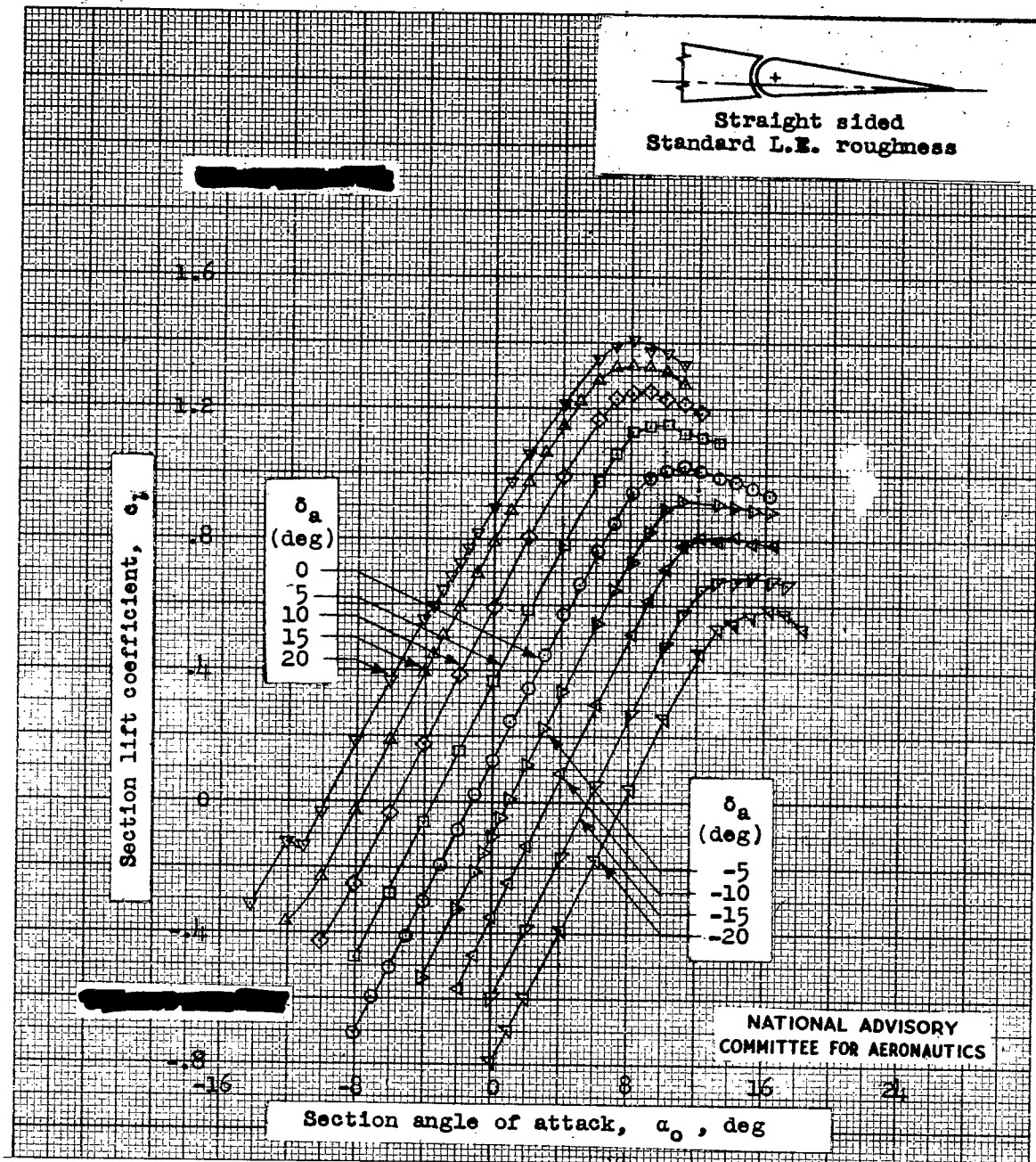


Figure 13.- Lift characteristics of an NACA 65₁-210 airfoil section equipped with a sealed-gap 0.20c plain aileron with straight sides. Standard leading-edge roughness; $R = 9 \times 10^6$; test, IDT 864.

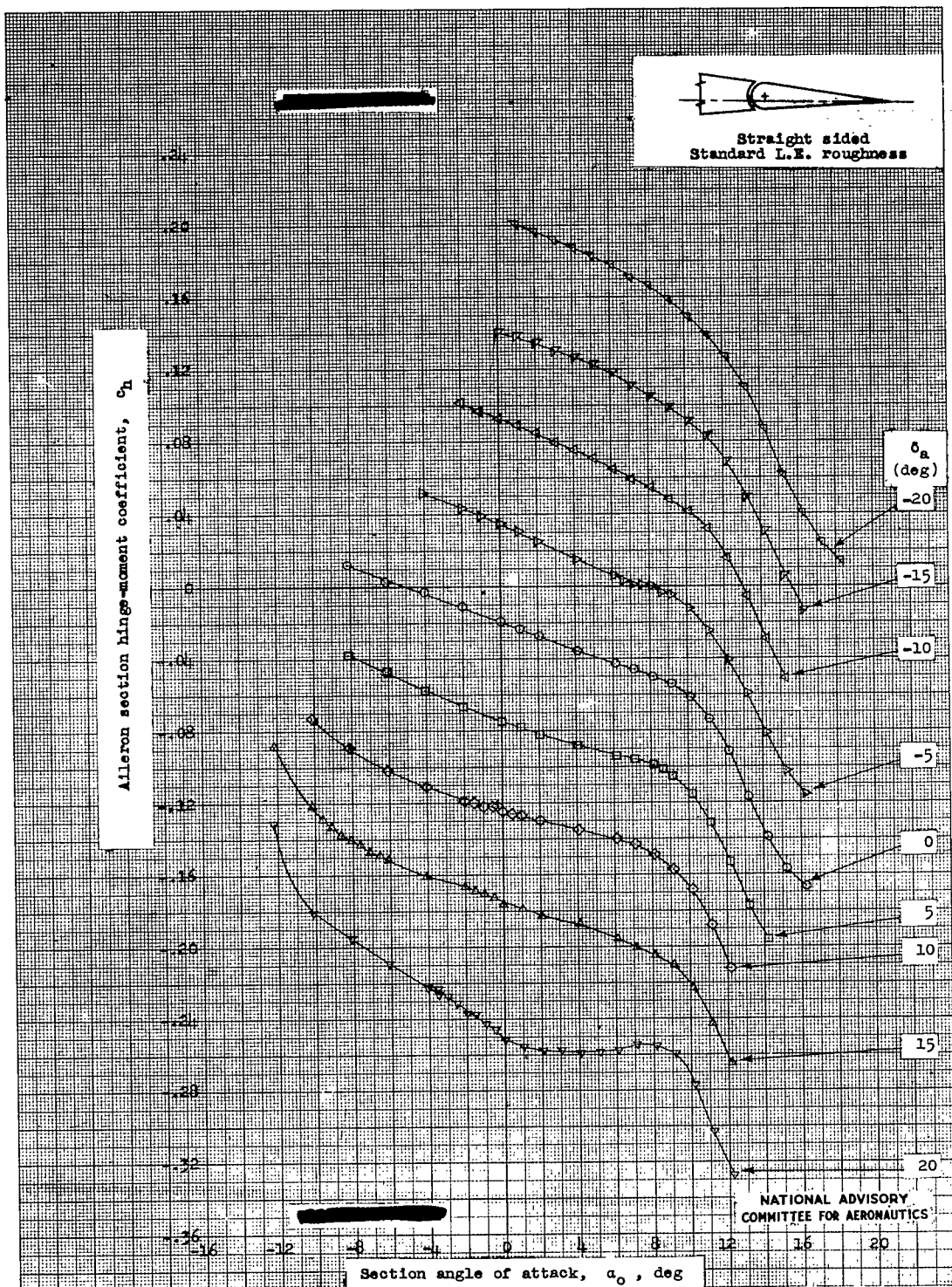


Figure 14.- Hinge-moment characteristics of a sealed-gap 0.20c plain aileron with straight sides on an NACA 65₁-210 airfoil section having standard leading-edge roughness. $R = 9 \times 10^6$; test, IDT 863.

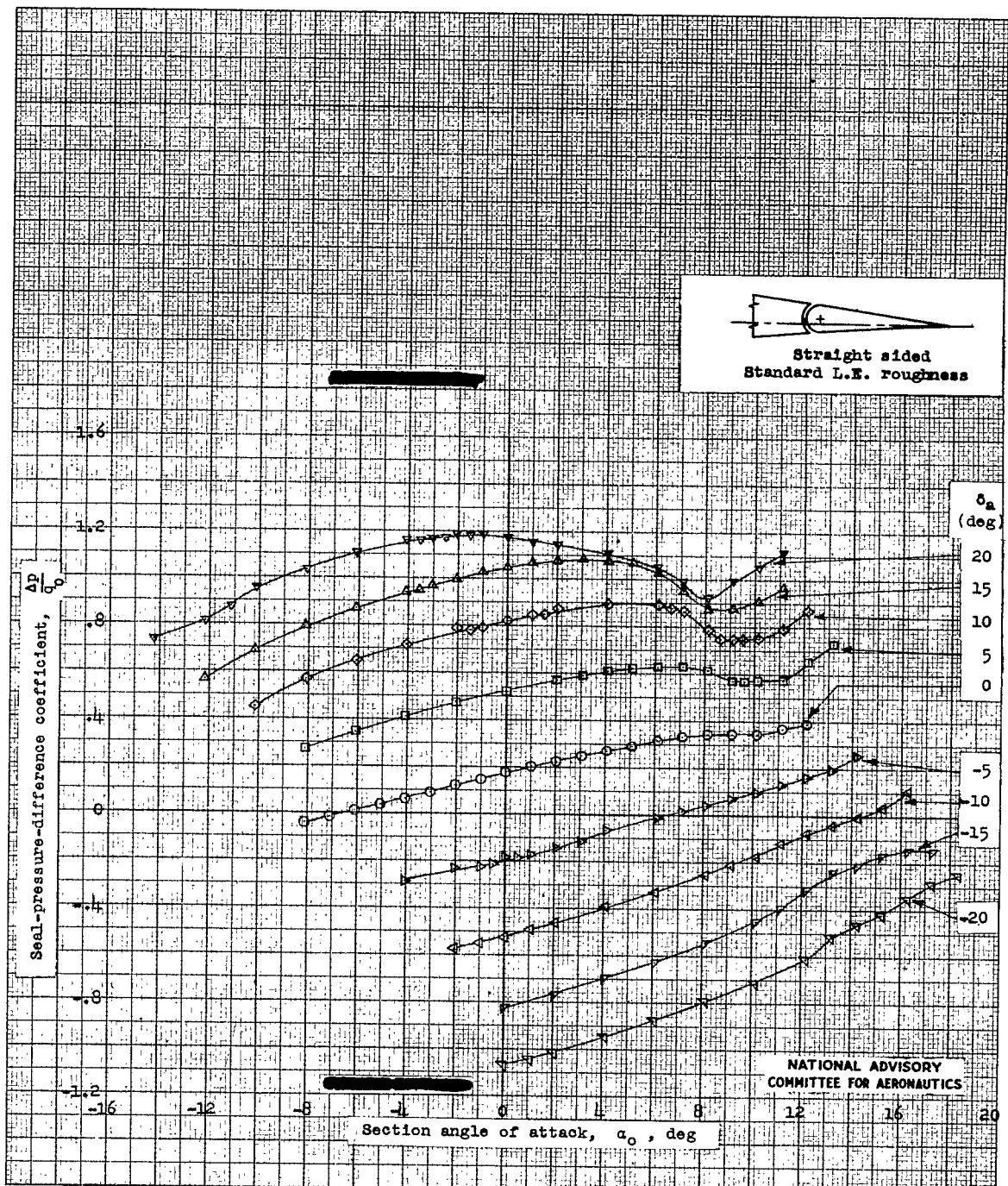


Figure 15.- Pressure difference across the gap seal of a 0.20c plain aileron with straight sides on an NACA 651-210 airfoil section having standard leading-edge roughness. $R = 9 \times 10^6$; test, TDT 864.

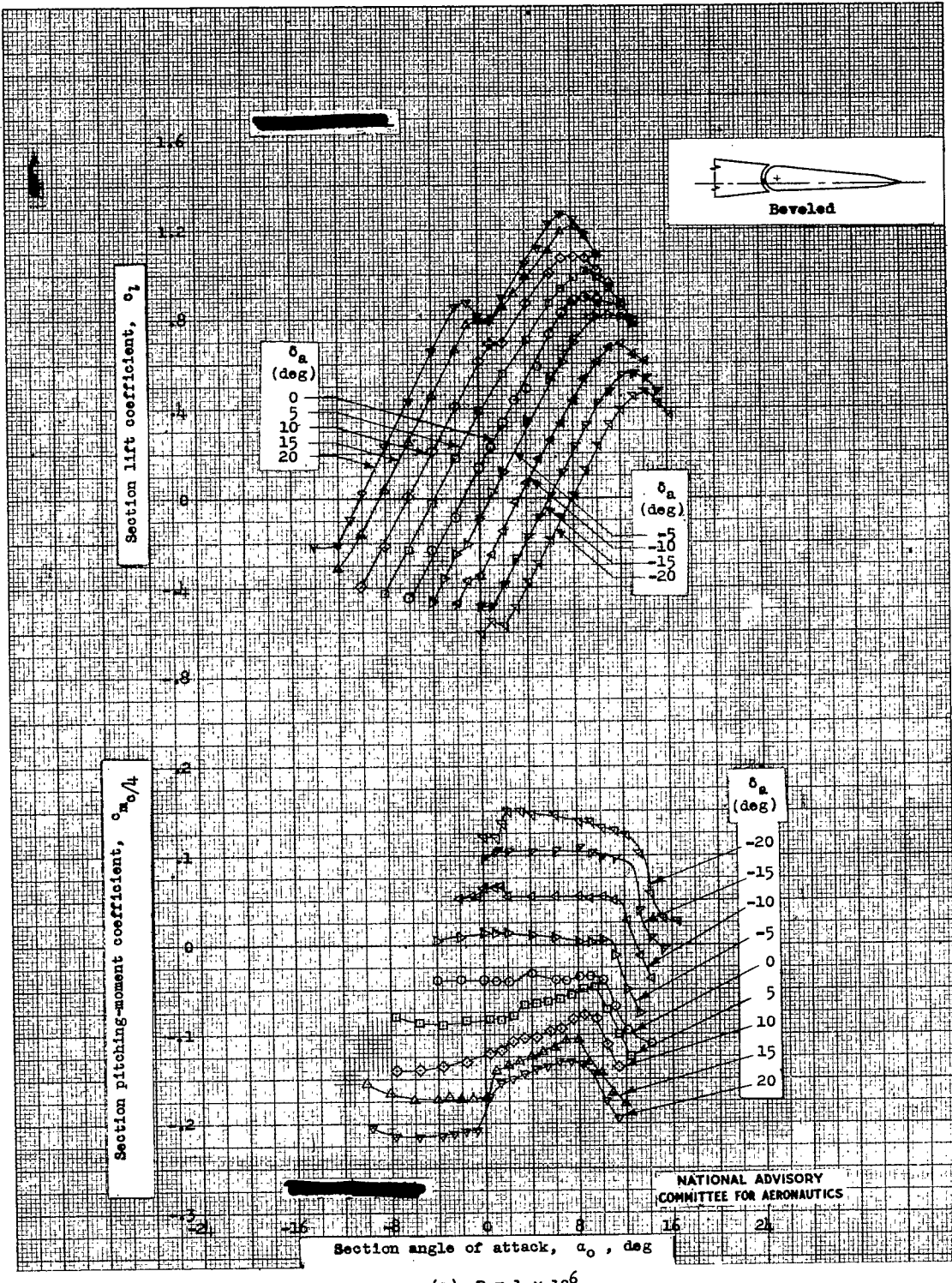
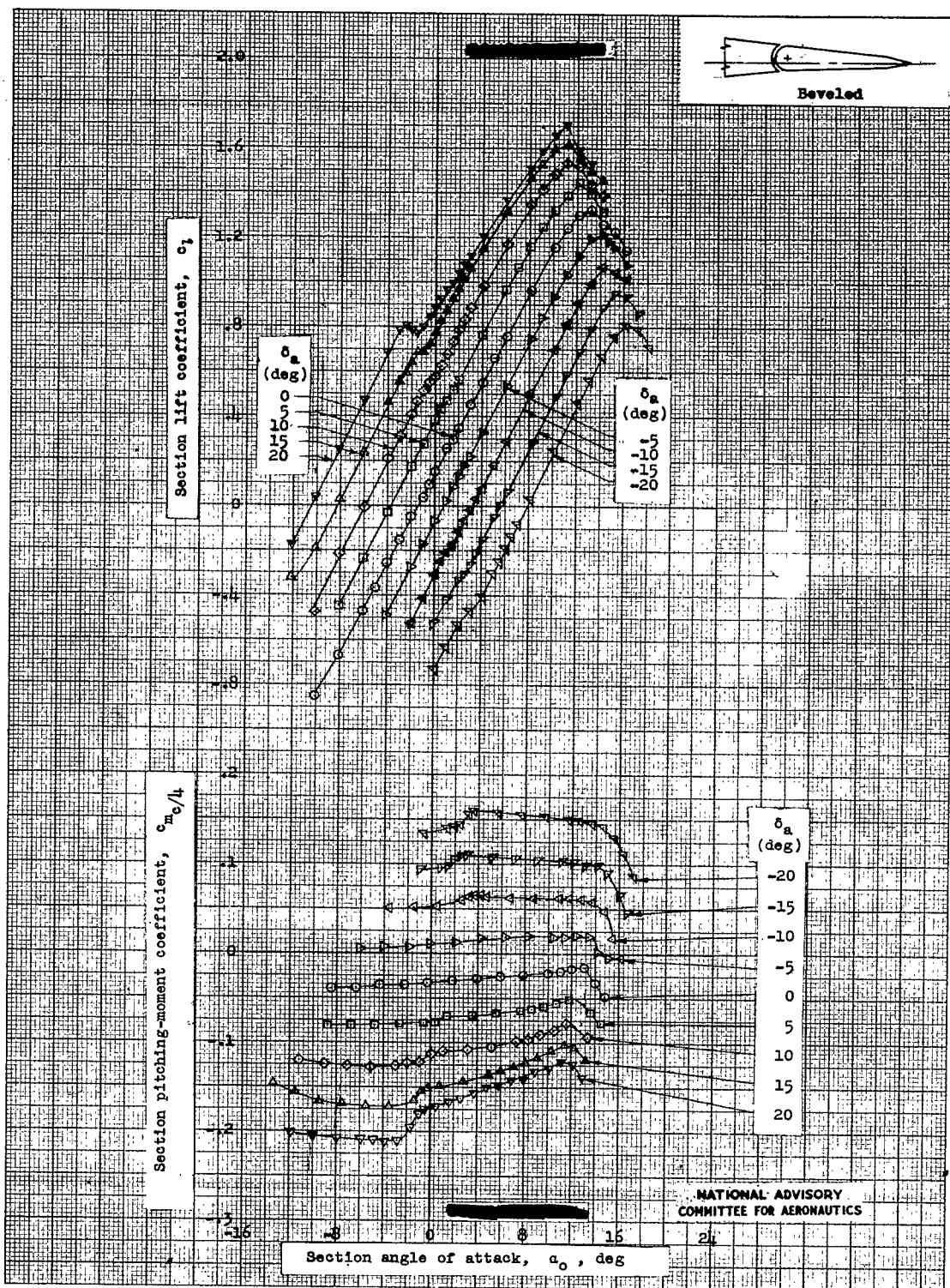


Figure 16a. Lift and pitching-moment characteristics of an NACA 651-210 airfoil equipped with a sealed-gap 0.20c plain aileron with beveled trailing edge. Tests, IDT 858, 859.



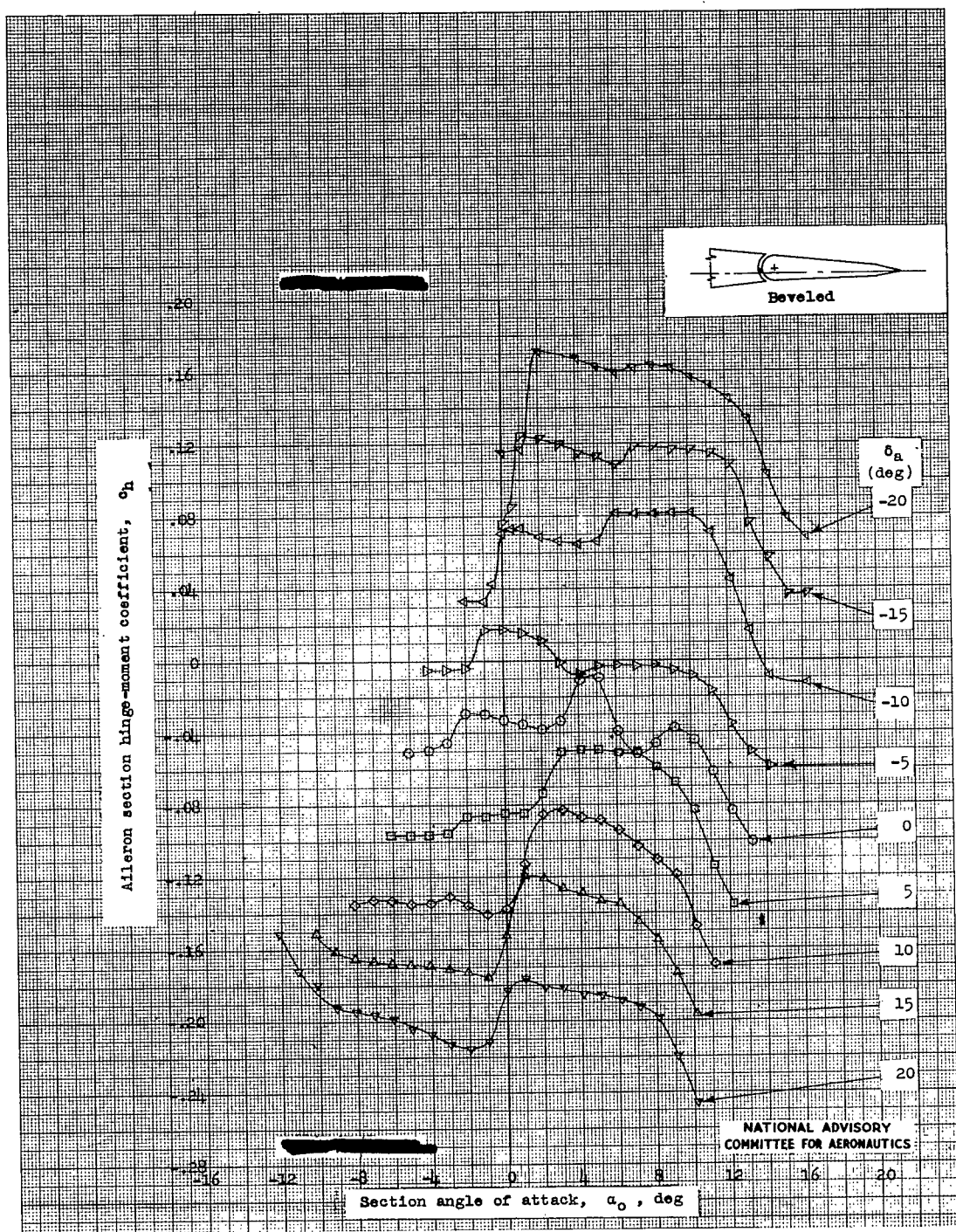
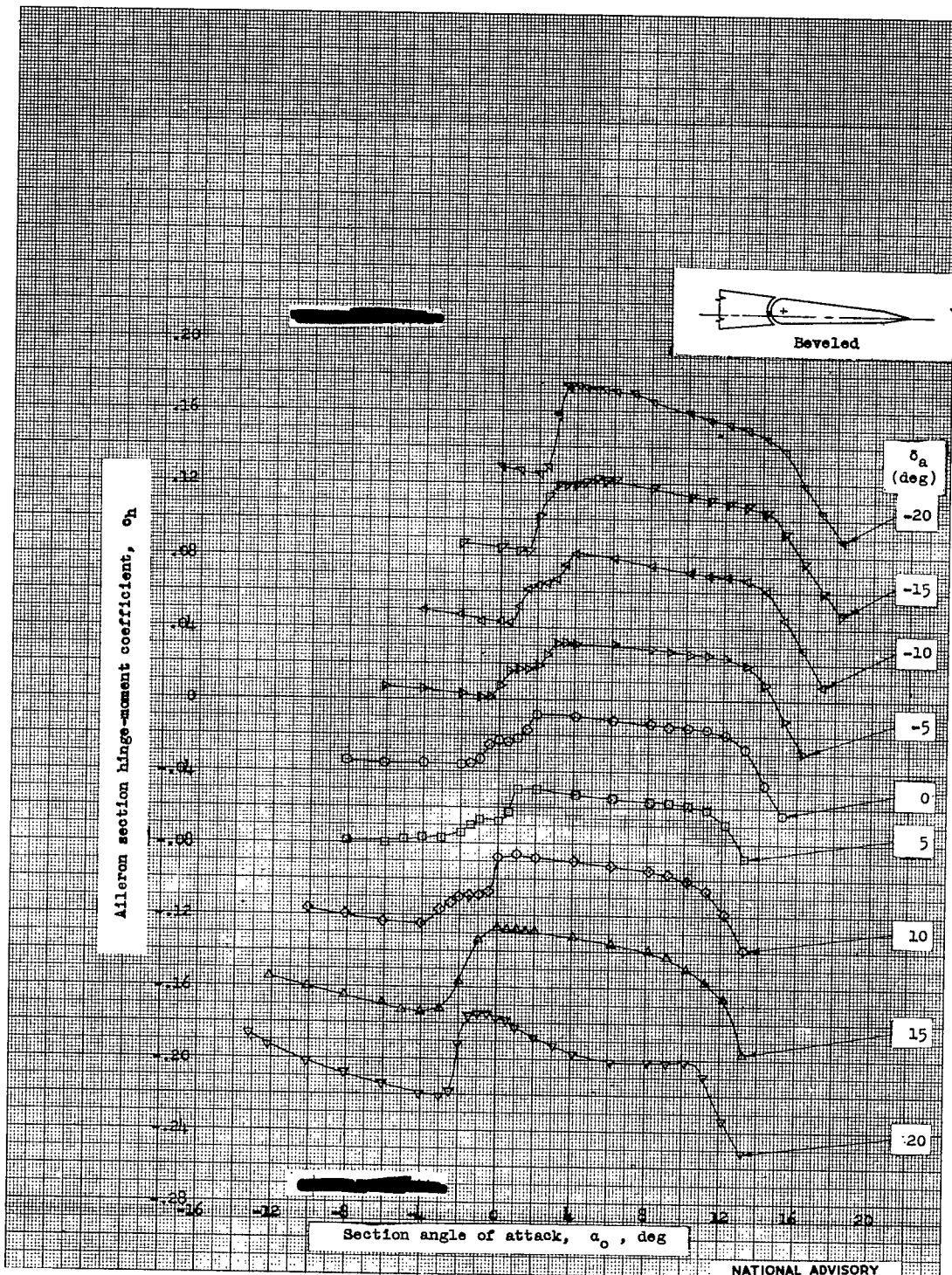
(a) $R = 1 \times 10^6$.

Figure 17.- Hinge-moment characteristics of a sealed-gap 0.20c plain aileron with beveled trailing edge on an NACA 65₁-210 airfoil section. Test, TDT 862.



NATIONAL ADVISORY
COMMITTEE FOR AERONAUTICS

(b) $R = 9 \times 10^6$.

Figure 17.- Concluded.

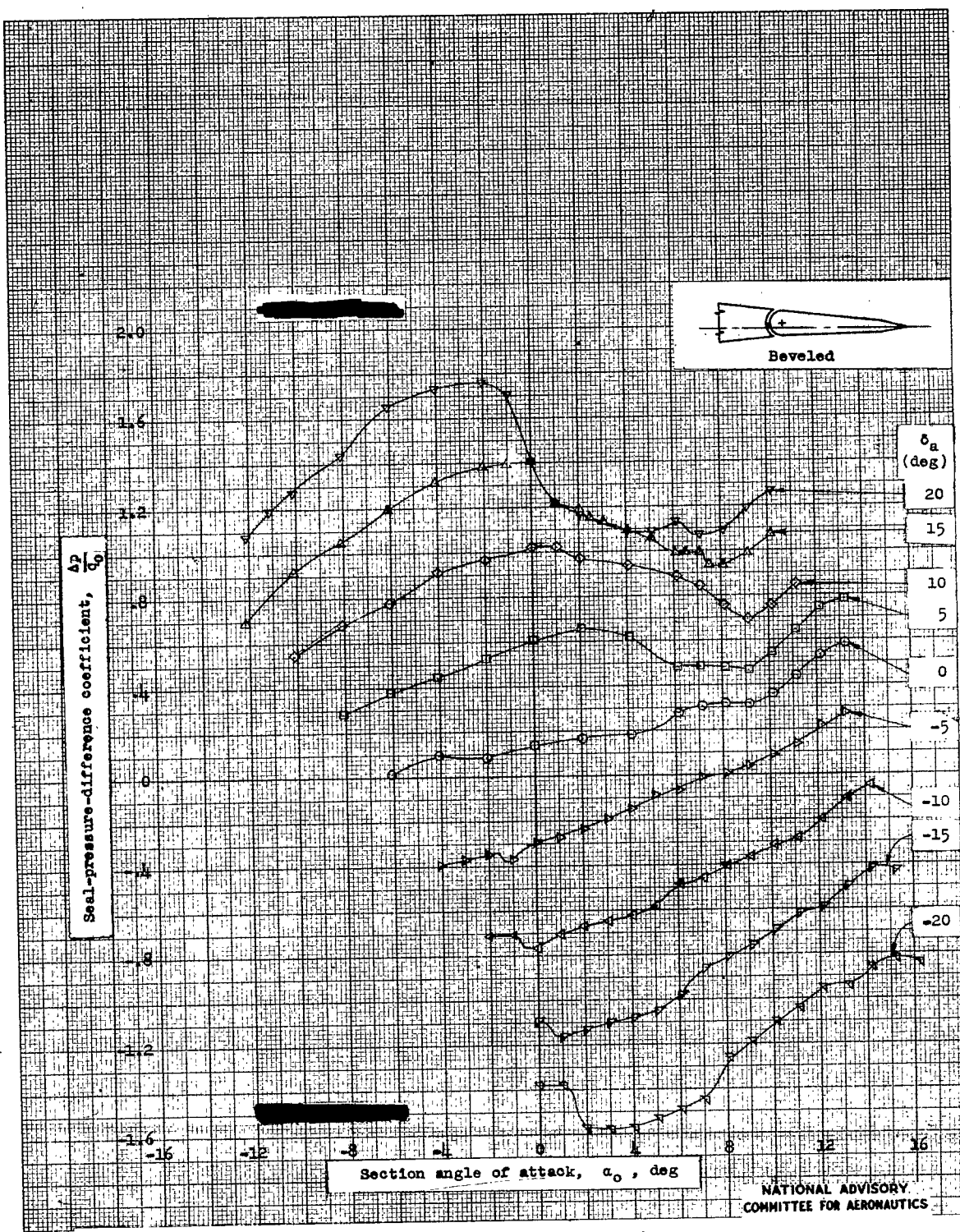
(a) $R = 1 \times 10^6$.

Figure 18.- Pressure difference across the gap seal of a 0.20c plain aileron with beveled trailing edge on an NACA 65-210 airfoil section. Test, TDT 859.

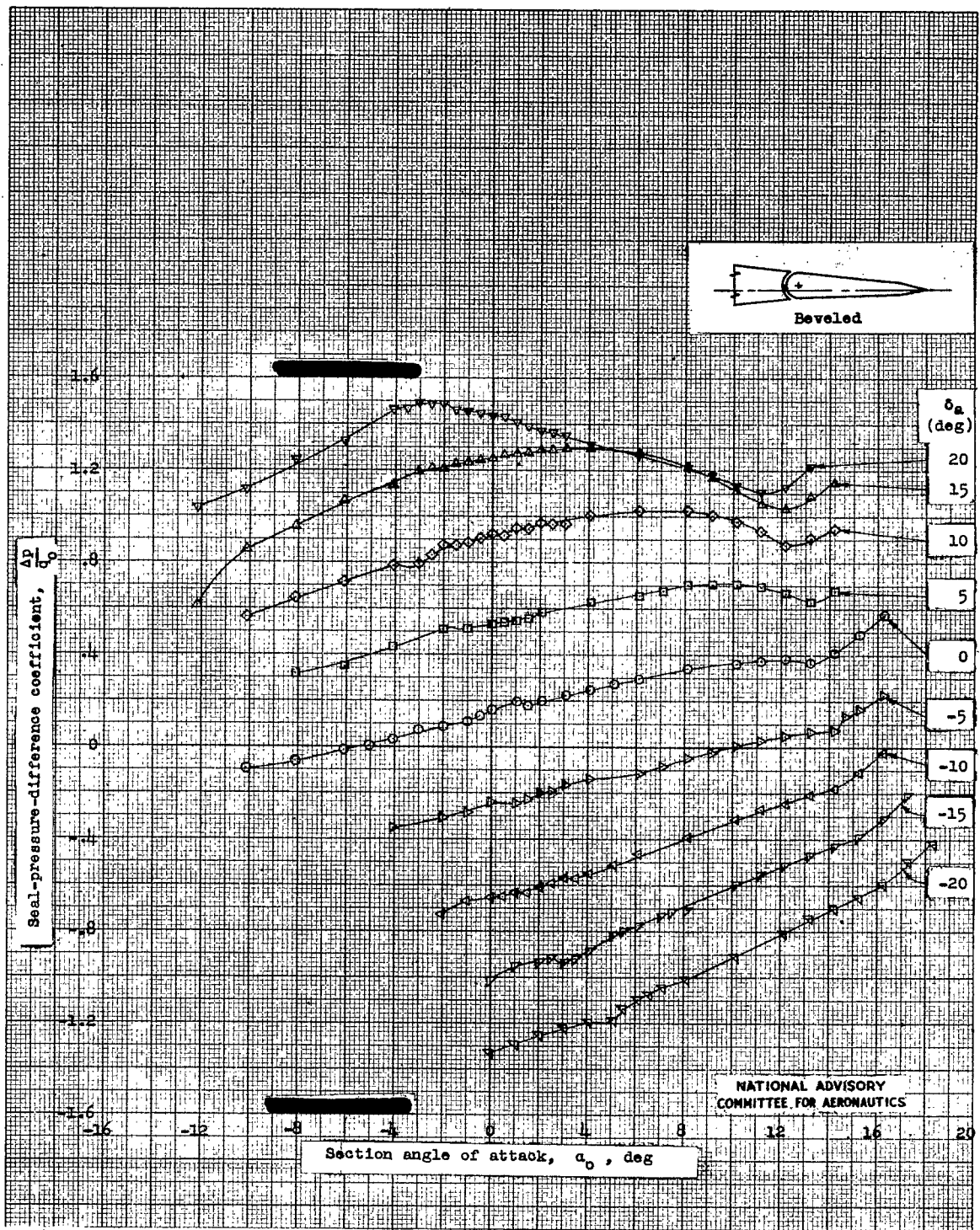
(b) $R = 9 \times 10^6$.

Figure 18 .- Concluded.

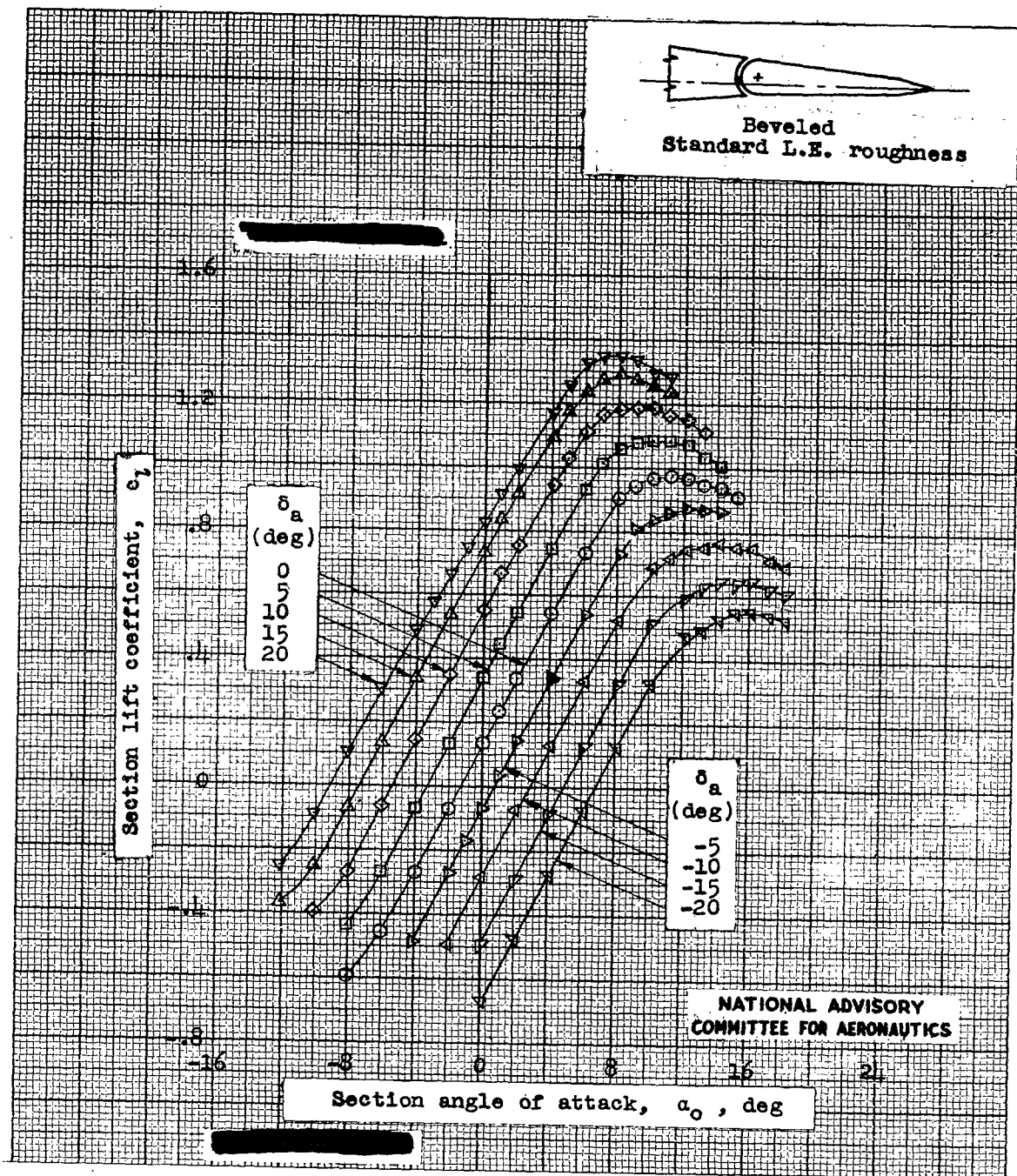


Figure 19.- Lift characteristics of an NACA 65₁-210 airfoil section equipped with a sealed-gap 0.20c plain aileron with beveled trailing edge. Standard leading-edge roughness; $R = 9 \times 10^6$; test, TDT 866.

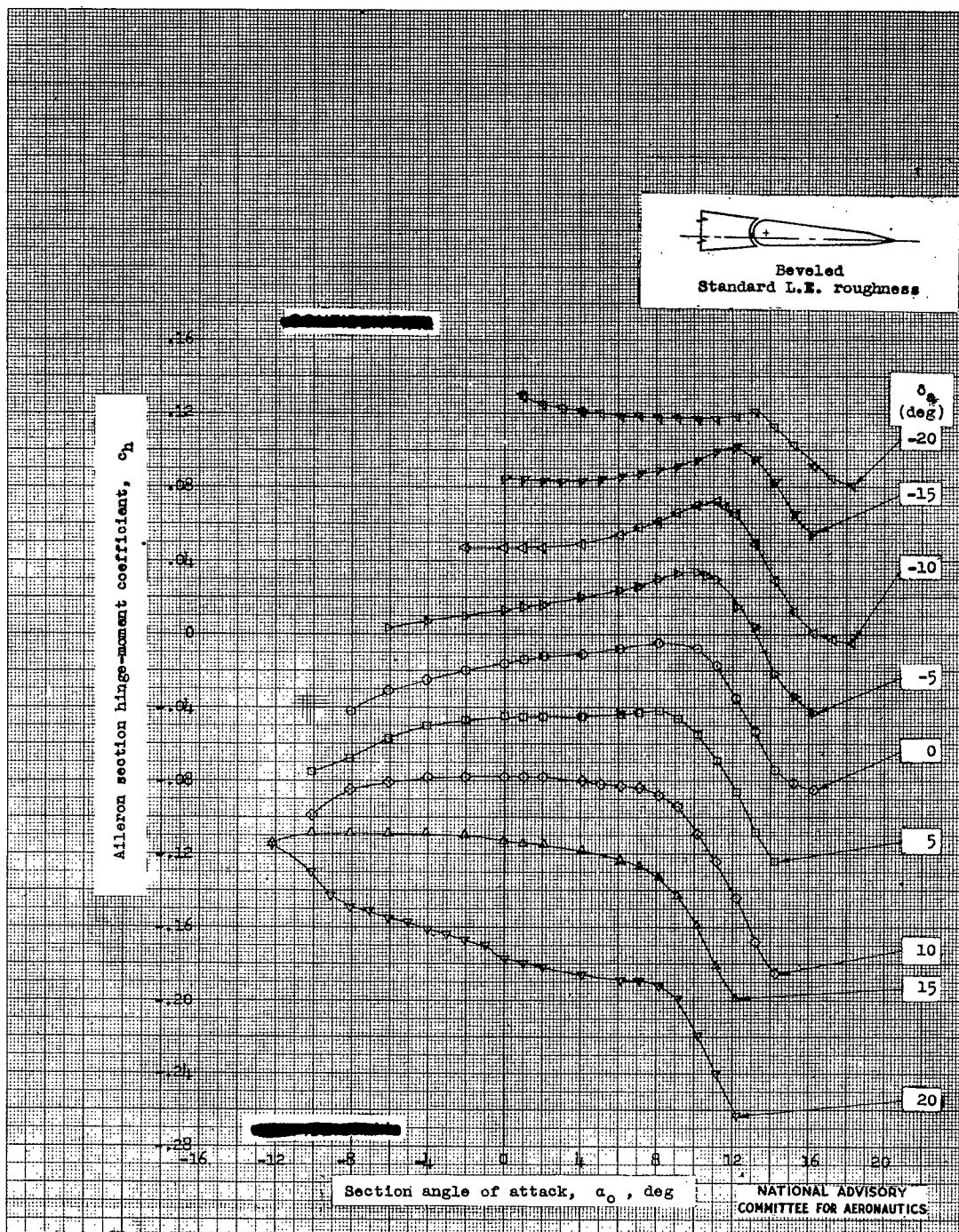


Figure 20.- Hinge-moment characteristics of a sealed-gap 0.20c plain aileron with beveled trailing edge on an NACA 651-210 airfoil section having standard leading-edge roughness. $R = 9 \times 10^6$; test, TDT 865.

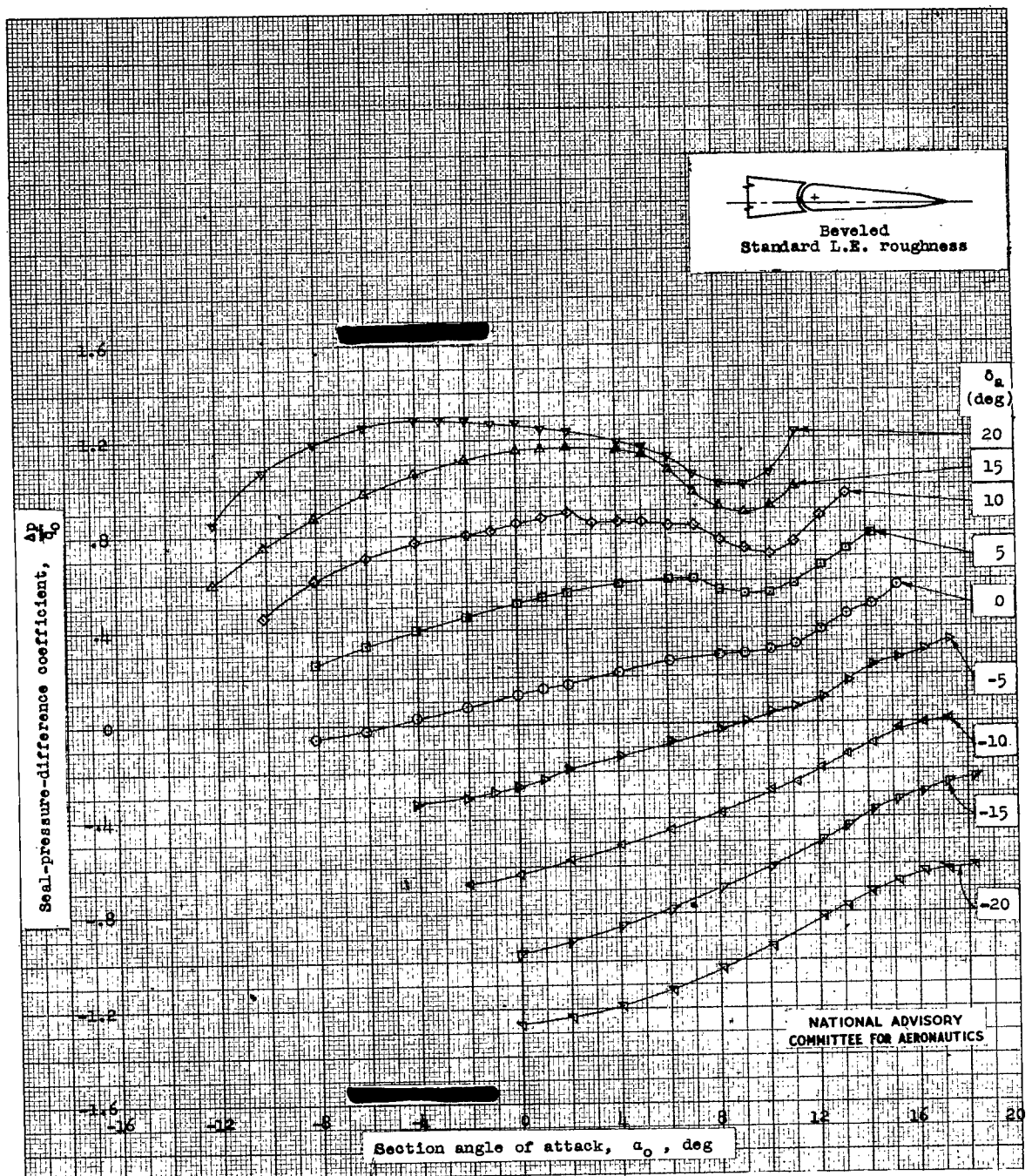
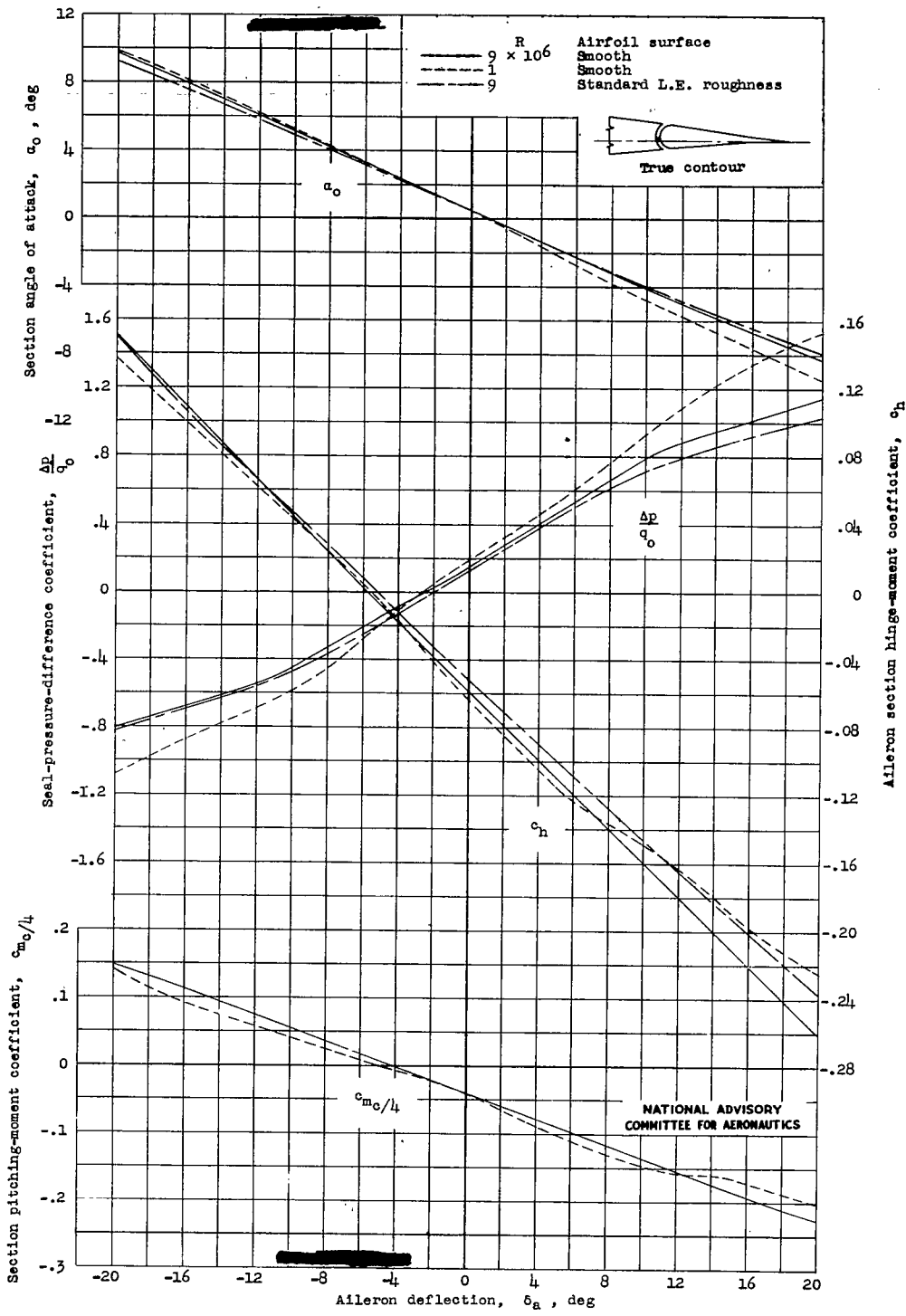
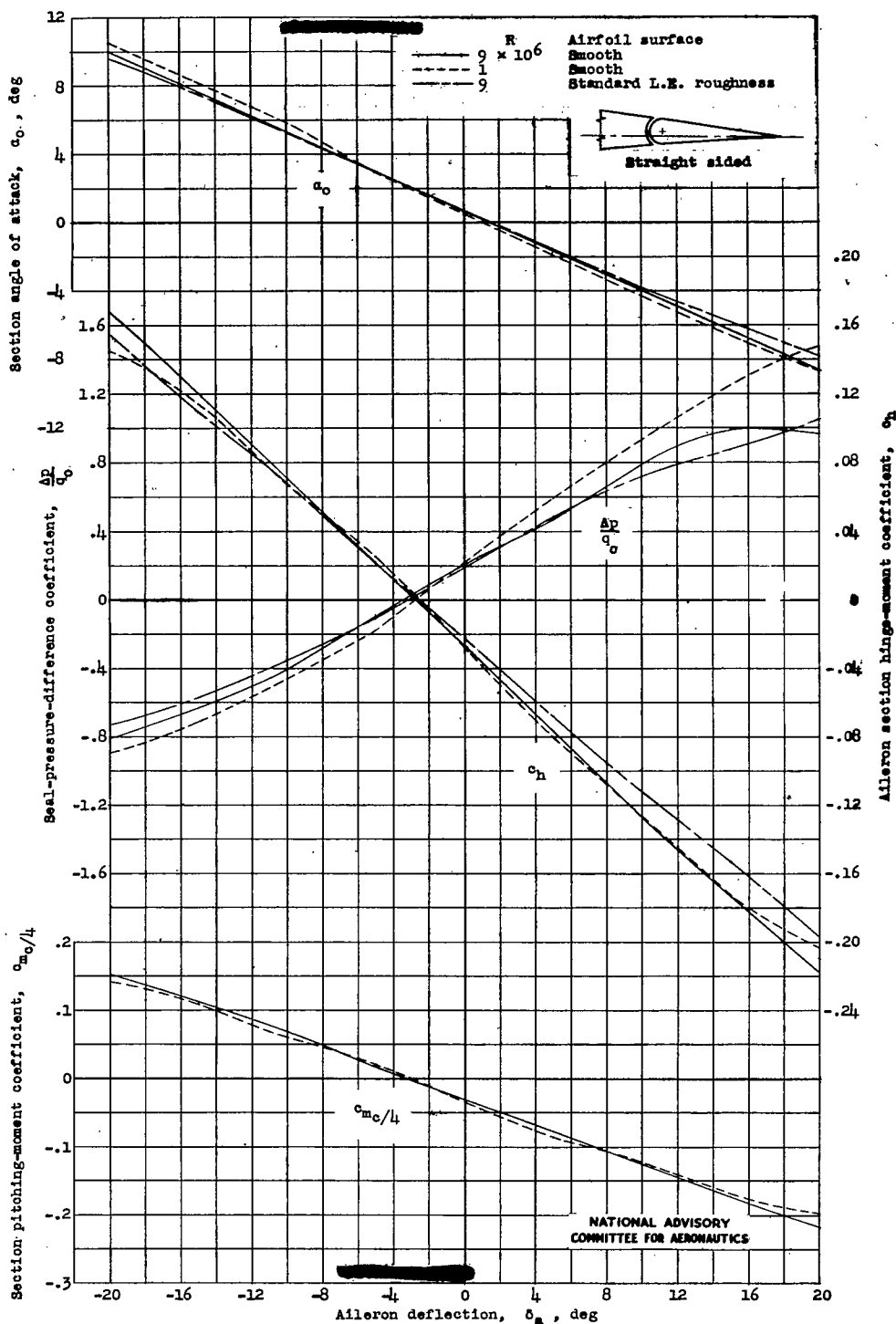


Figure 21.- Pressure difference across the gap seal of a 0.20c plain aileron with beveled trailing edge on an NACA 65-210 airfoil section having standard leading-edge roughness. $R = 9 \times 10^6$; test, IDT 866.



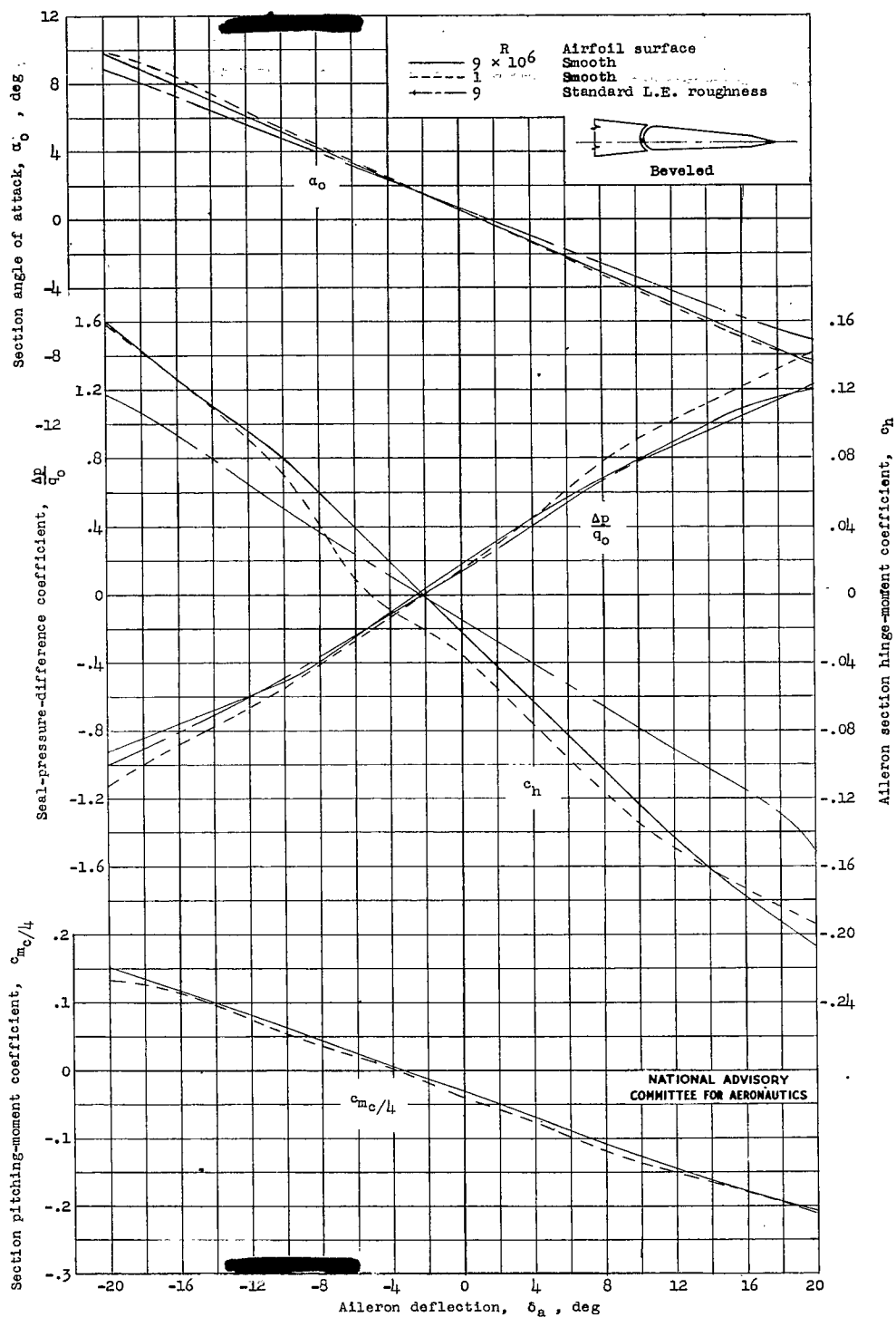
(a) True-contour aileron.

Figure 22.- Variation of aerodynamic characteristics with aileron deflection at a constant section lift coefficient of 0.20 for an NACA 65₁-210 airfoil section equipped with three interchangeable sealed-gap 0.20c plain ailerons of different contour.



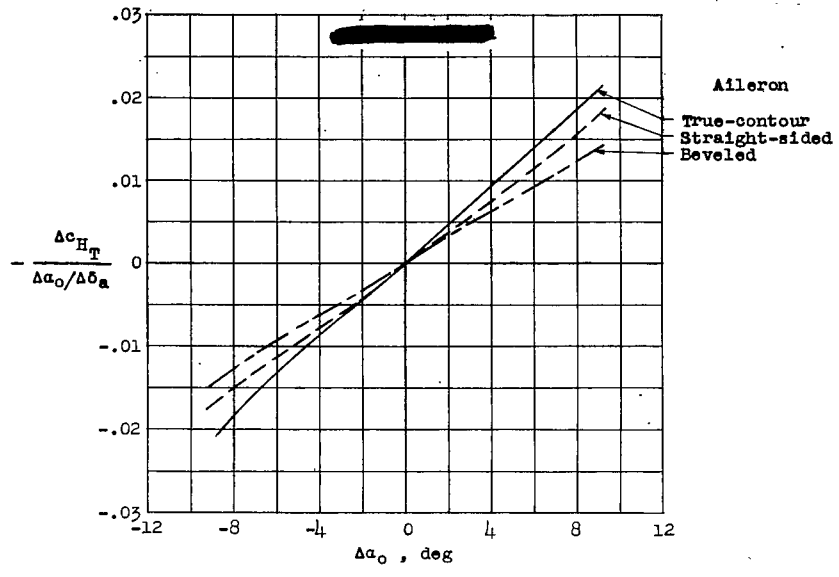
(b) Straight-sided aileron.

Figure 22.- Continued.

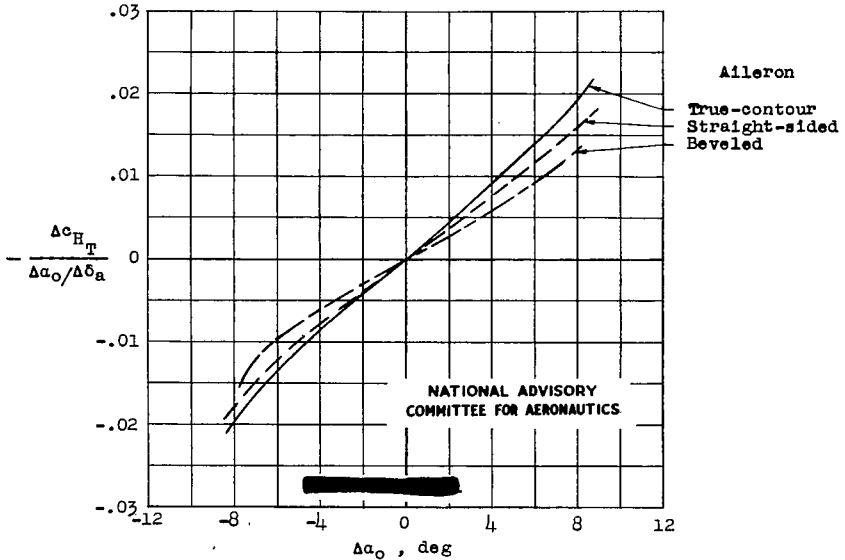


(c) Beveled aileron.

Figure 22c Concluded.



(a) Smooth airfoil.



(b) Airfoil with standard leading-edge roughness.

Figure 23.- Variation of the hinge-moment parameter $\frac{\Delta c_{H_T}}{\Delta a_0 / \Delta \delta_a}$ with equivalent change in

section angle of attack required to maintain a constant section lift coefficient of 0.20 for deflection of sealed-gap 0.20c plain ailerons of different contour on an NACA 65₁-210 airfoil section. $R = 9 \times 10^6$.

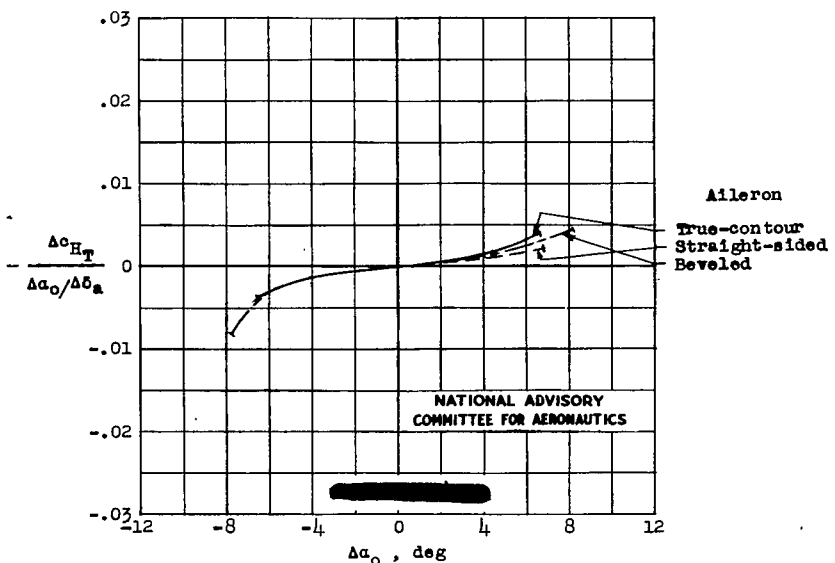
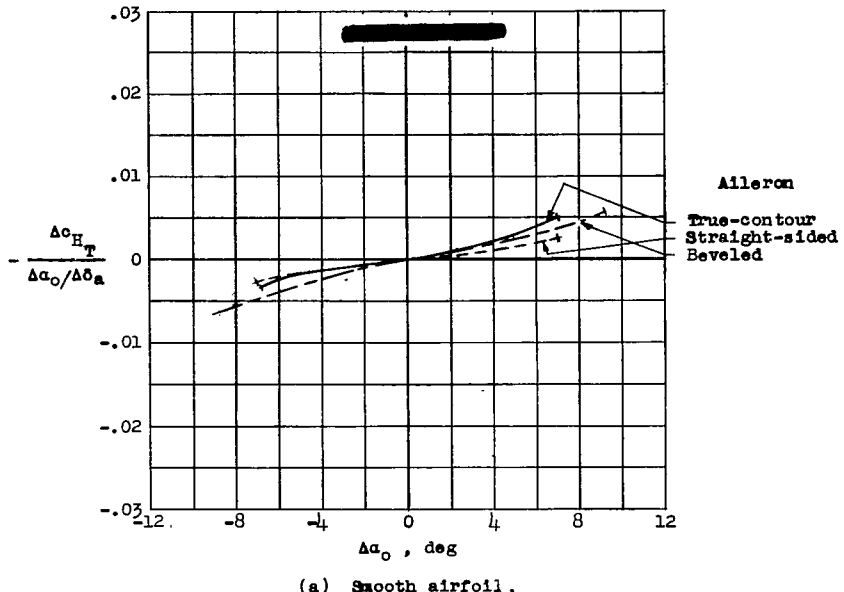
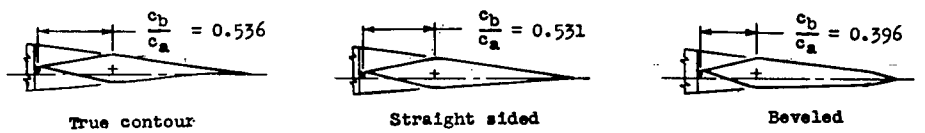


Figure 24.- Variation of the hinge-moment parameter $\frac{\Delta c_{H_T}}{\Delta \alpha_0 / \Delta \delta_a}$ with equivalent change

in section angle of attack required to maintain a constant section lift coefficient of 0.20 for deflection of sealed 0.20c internally balanced ailerons of different contours on an NACA 65₁-210 airfoil section. $R = 9 \times 10^6$.

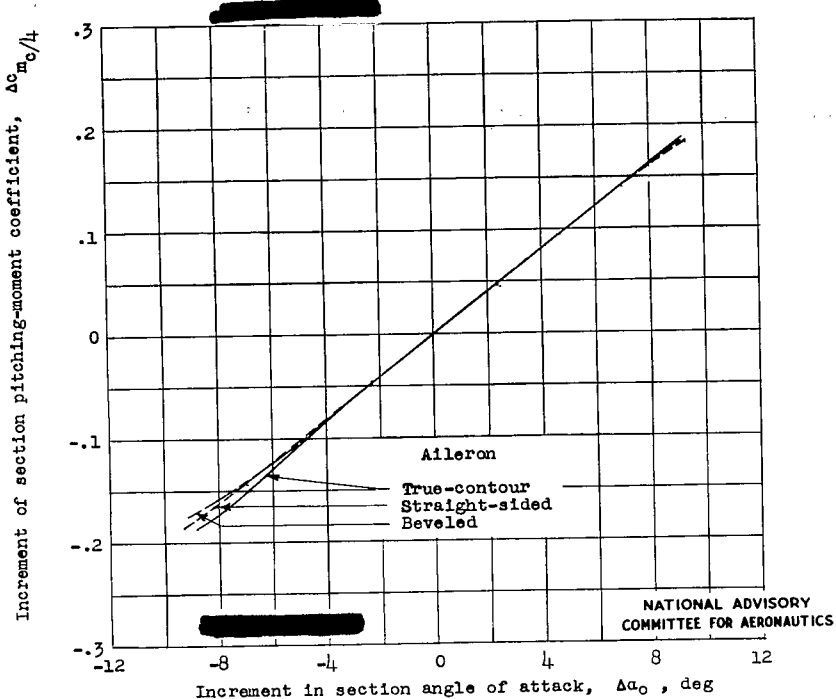


Figure 25.- Variation of increment of section pitching-moment coefficient of an NACA 651-210 airfoil section with equivalent change in section angle of attack required to maintain a constant section lift coefficient of 0.20 for deflection of the three sealed-gap 0.20c plain ailerons of different contour. $R = 9 \times 10^6$.

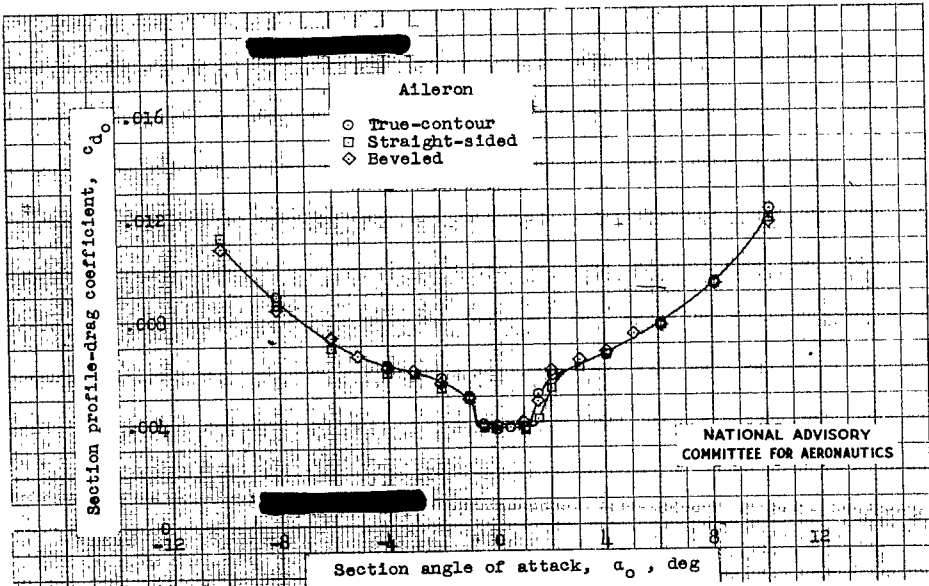


Figure 26.- Effect of aileron contour on the section profile-drag coefficient of a NACA 651-210 airfoil section equipped with sealed-gap 0.20c plain ailerons. $\delta_a = 0^\circ$; $R = 9 \times 10^6$.

LANGLEY RESEARCH CENTER



3 1176 01363 9035